COPY 1 of 1 COPIES

LIFT ON INCLINED BODIES OF REVOLUTION IN HYPERSONIC FLOW

by

G. Grimminger, E. P. Williams & G. Young

P-87

REV. April 17, 1950

The RAND Corporation
1700 MAIN ST • SANTA MONICA • CALIFORNIA

DISCLAIMER NOTICE

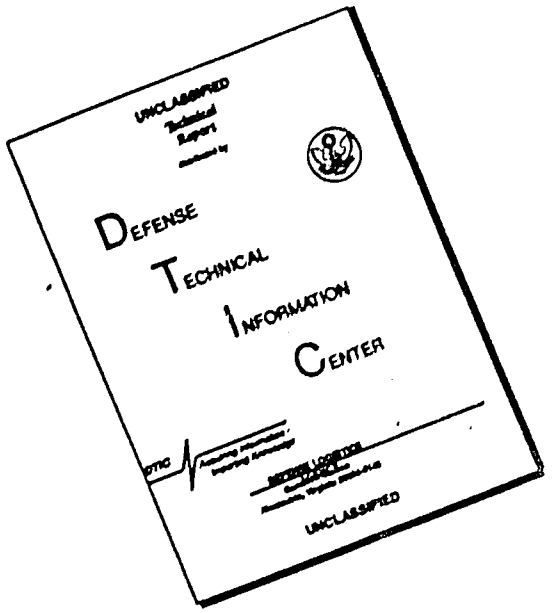

THIS DOCUMENT IS BEST QUALITY AVAILABLE. THE COPY FURNISHED TO DTIC CONTAINED A SIGNIFICANT NUMBER OF PAGES WHICH DO NOT REPRODUCE LEGIBLY.

SYMBOLS

A = cross-section area

b = unit vector tangent to a circular parallel

C_N = normal force coefficient = $N/q_0\pi r_B^2$

C_N' = local normal force coefficient = $dC_N/d(x/d_B)$

C_p = $(p - p_0)/q_0$ = pressure coefficient

C_X = axial force coefficient = $X/q_0\pi r_B^2$

C_X' = local axial force coefficient = $dC_X/d(x/d_B)$

d = diameter

ℓ = length

M_0 = free stream Mach number

$\dot{m}$ = rate of mass flow

N = normal force — that is, force normal to longitudinal axis of body

n = unit vector normal to surface, positive inward

p = static pressure

q = $\frac{1}{2}\rho V^2$ = dynamic pressure

R = radius of normal curvature of a streamline

r = radius

S = surface area

t = unit vector tangent to a meridian

V = velocity

V_0 = free stream velocity vector

V_s = velocity of flow over the surface of the body

X = axial force — that is, force in direction of longitudinal axis of body

x = distance along longitudinal axis of body

α = angle of attack

β = angular position of a point on the surface of the body

β_u = upper limit of integration around a circular parallel

γ = angle between body streamline and a meridian

δ_B = thickness of body layer

η = angle between V_0 and n

θ = angle between t and the longitudinal axis of the body

θ_v = semi-vertex angle of cone

ρ = mass density

ρ_B = density in body layer

SUBSCRIPTS

$( )_B$ = based on maximum body dimensions

$( )_c$ = centrifugal force values

$( )_C$ = converging or boattail section

$( )_D$ = nose or diverging section

$( )_e$ = refers to expansion flow

$( )_i$ = impact values

$( )_S$ = straight or cylindrical section

$( )_0$ = based on free stream conditions

P-67
Rev.Apr.1950

LIFT ON INCLINED BODIES OF REVOLUTION IN HYPERSONIC FLOW

by

G. Grimminger*, E. P. Williams', and G. B. W. Young‡

The RAND Corporation

SUMMARY

The importance of body lift lies in the fact that at moderate angles of attack and high Mach number it can constitute an appreciable part of the total lift of a winged missile. In this paper an attempt has been made to analyze body lift in hypersonic flow by an approximate method and, together with a correlation of existing experimental data, to indicate the probable variation of body lift over a wide range of Mach number extending from low supersonic to hypersonic. The method of analysis of hypersonic flow over inclined bodies of revolution employed herein has been denoted as the hypersonic approximation. It is an improvement on the Newtonian corpuscular theory of aerodynamics since it considers the centrifugal forces resulting from the curved paths of the air particles in addition to the impact (Newtonian) forces.

*Physical Scientist; now with the Department of Defense, Washington, as Scientific Warfare Advisor.

'Aerodynamics Engineer

‡Research Engineer

I. INTRODUCTION

In the field of guided missiles, investigations of possible performance will inevitably lead to the consideration of flight at higher and higher Mach numbers. Although for some missiles the Mach number $M_0 = 5$ might be considered as the upper end of the speed range, for missiles of a different category the high speed range of flight can conceivably extend to $M_0 = 20$ or 25. As far as wing aerodynamics is concerned, for supersonic speeds up to $M_0 = 5$ the wing lift may be obtained with satisfactory accuracy by means of the linearized supersonic wing theories, and at higher Mach numbers satisfactory results are obtained on the basis of two-dimensional gas dynamics. However, this is not at all the case for strictly three-dimensional flow such as that over a yawed body of revolution. In the usual application of linearized theories in two- and three-dimensional flow, wherein the higher order terms are neglected throughout for the sake of consistency, good solutions can be obtained for supersonic wings but not for body lift. Furthermore, these linearized solutions are subject to Mach number limitations. On the other hand, reliable theoretical lift results exist for cones at the present time.(1), (2) This yawed cone theory gives the exact initial normal force slope which is practically independent of Mach number and in excellent agreement with the hypersonic approximation of the present paper as shown by Fig. 1; agreement with some experimental data is shown in Fig. 2. Less is known about the lift of an ogive, however, and still less about the lift of a cylinder following either a cone or ogive.

In view of the fact that at the higher Mach numbers body lift can constitute an appreciable part of the total lift of a winged missile, an attempt has been made to analyze body lift in hypersonic flow by an approximate method and, together with an analysis of existing experimental data, to indicate the probable variation of body lift over a wide range of Mach number extending from low supersonic to hypersonic. First, the Newtonian analysis is presented for

an arbitrary inclined body of revolution. The resulting forces on a cone and cylinder are then given. Centrifugal force effects reduce the cylinder normal force resulting from the Newtonian analysis by approximately ten percent. Corresponding effects for slender cones and ogives are less for the angle of attack range of general interest ($\alpha<2\theta_c$) so for practical purposes the Newtonian analysis needs no modification for predicting the lift on the nose of a body of revolution at very high Mach numbers. A qualitative discussion of the pressures on cone and cylinder areas situated in regions of expansion flow at hypersonic speeds is then presented. It serves as a guide for extending the results of the following correlation of experimental lift data through the hypersonic region to the hypersonic approximation values. A more detailed discussion and analysis of centrifugal force effects are given in the Appendix.

II. THE NEWTONIAN (IMPACT) AERODYNAMIC FORCES ON A YAWED BODY OF REVOLUTION

In view of the general lack of exact gas dynamic results for three-dimensional flow it is important to realise that valuable results concerning the lift on a pointed body of revolution can be obtained from the relatively simple theory of Newtonian aerodynamics. At high supersonic Mach numbers, particularly when the angle of attack is appreciable, the gas pressure forces on a body may be approximated in a simple manner on the basis of the concept of Newtonian flow. (3-5) In Newtonian flow it is assumed that the gas stream maintains its speed and direction unchanged until it strikes the solid surface exposed to the flow, whereupon it loses the component of momentum normal to the surface and moves along the surface with the tangential component of momentum unchanged. Thus, in this concept the shock wave is assumed to lie on, or follow, the surface of the body. The Newtonian approximation does not specify the pressure on surfaces which do not "see" the flow, that is, surfaces on which gas dynamics would predict expansion flow. For a flat plate inclined at an angle α to the flow, the Newtonian pressure coefficient on the lower surface is

$$C_p \equiv \frac{p - p_0}{q_0} = 2 \sin^2 \alpha, \tag{1}$$

where p_0 denotes free-stream pressure, and $q_0 = \frac{1}{2}\rho_0 V_0^2$ is the free-stream dynamic pressure.

The concept of Newtonian flow can also be approached from the exact two-dimensional gas dynamical equations by letting $M_0 \to \infty$. Considering a flat plate inclined to the flow, there will be shock flow over the lower surface and expansion flow over the upper surface. As the Mach number increases, the shock wave approaches closer and closer to the lower surface (leading to increasing pressures) and the amount of expansion increases on the upper surface (leading to decreasing pressures). In the limit when $M_0 = \infty$ both the pressure and the pressure coefficient on the upper

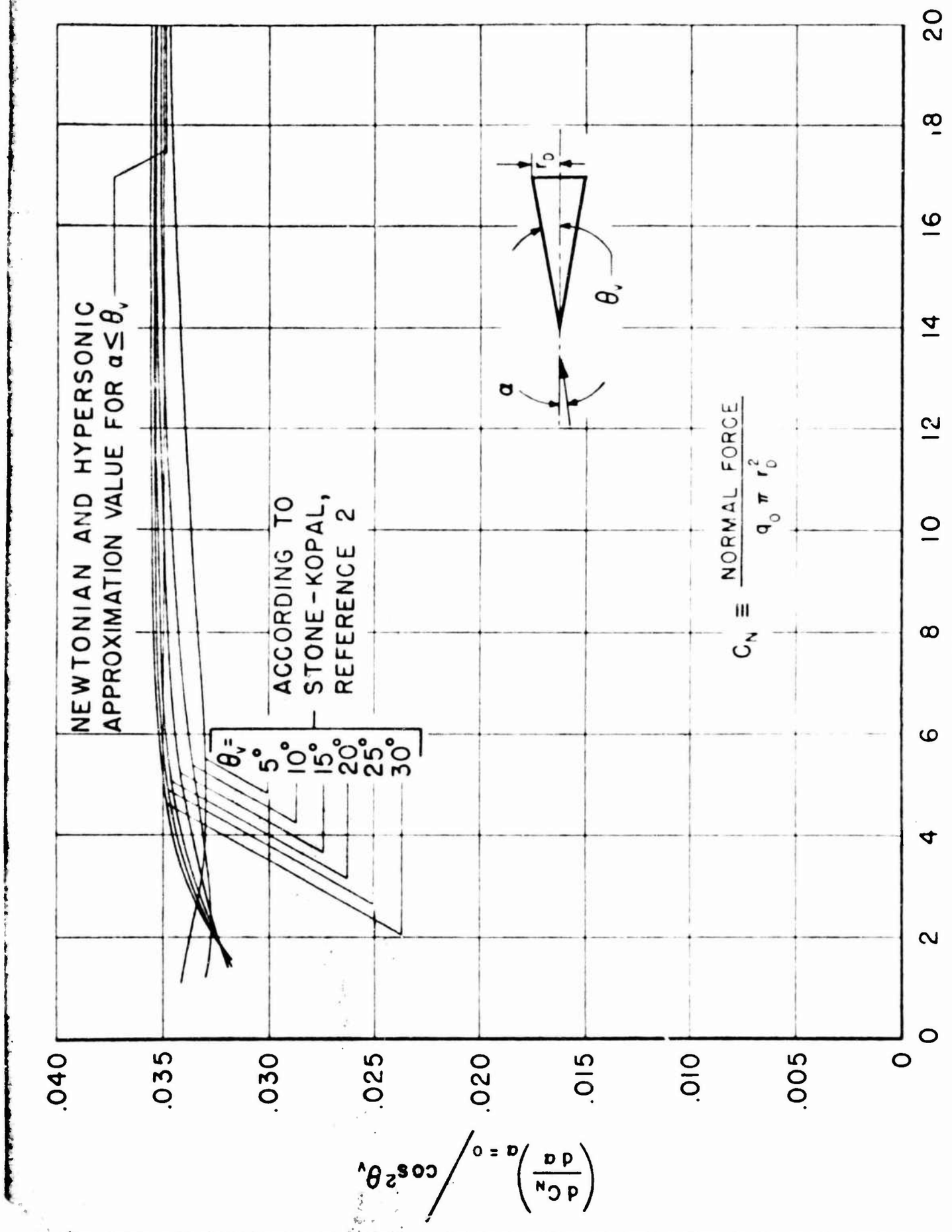

CONE NORMAL FORCE COEFFICIENT SLOPE vs MACH NUMBER

FIG. 1

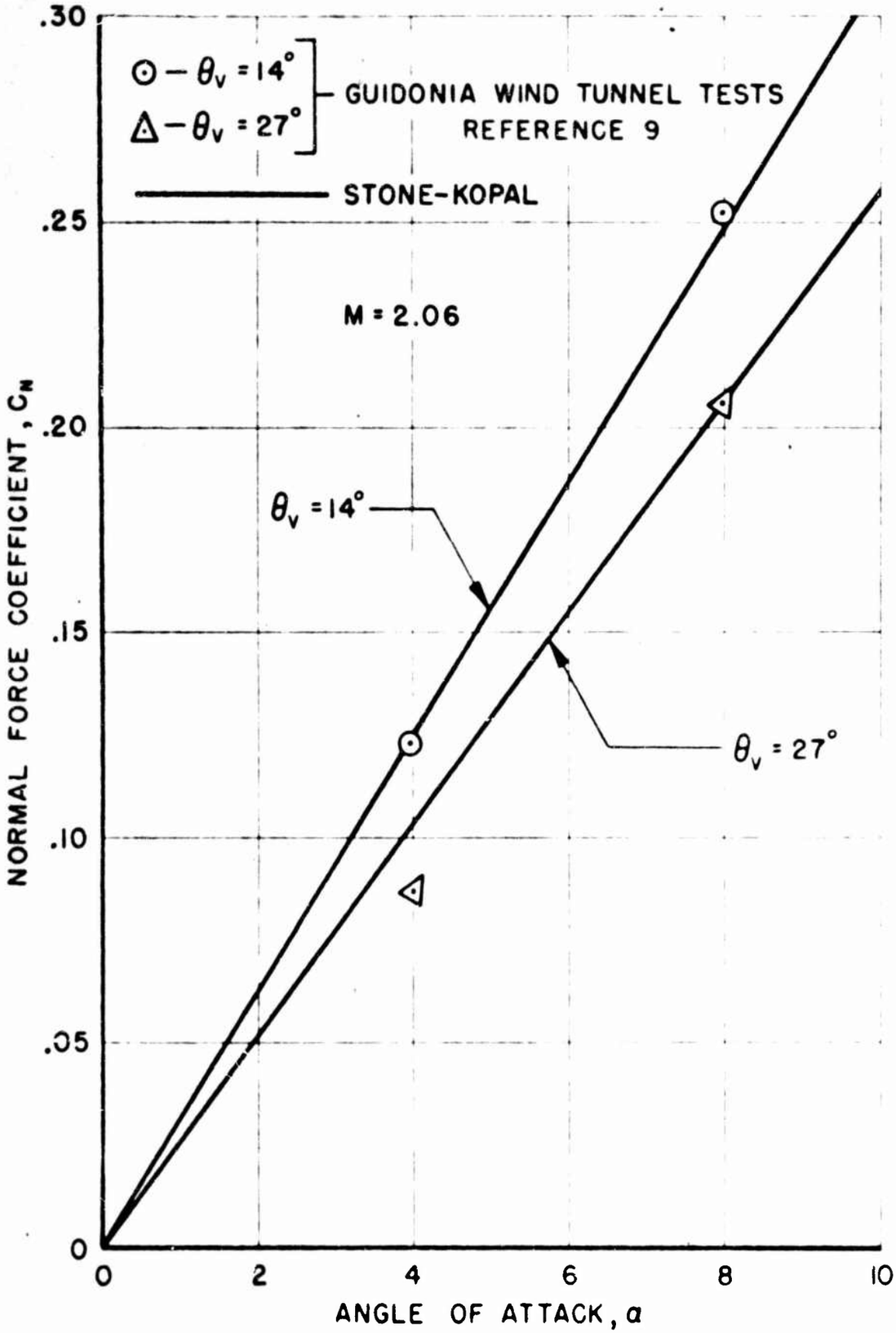

NORMAL FORCE COEFFICIENT FOR CONES

FIG. 2

surface becomes zero, and the pressure coefficient on the lower surface becomes (6)

$$C_p = (\gamma + 1) \sin^2\alpha = C_N \tag{2}$$

where γ is the ratio of the specific heats. Since the upper surface pressure coefficient is zero, Eq.(2) is also the expression for the normal force coefficient C_N. It is indicated in Ref. 4 that $\gamma \to 1$ as $M_0 \to \infty$, which brings Eq.(2) into agreement with the Newtonian result, Eq.(1). It is worth pointing out that for a given Mach number and angle of attack the Newtonian theory gives considerably better results for a three-dimensional body than for a two-dimensional body. Thus, the Newtonian hypersonic approximation for a pointed body of revolution, such as a cone for example, is surprisingly good and is much better than for a two-dimensional flat plate.

A. ARBITRARY BODY OF REVOLUTION

To derive the Newtonian pressure forces on a body of revolution of general shape, consider the body shown in Fig. 3 for which the longitudinal axis of symmetry is the positive x-axis. The angle of attack α is the angle in the xz-plane between the free-stream velocity vector V_0 and the positive x-axis. The y-axis is perpendicular to the xz-plane, forming a right-handed system of coordinates. Consider a differential element of surface area dS at an arbitrary point O' on the surface of the body and let x', y', z' denote a local right-handed system of coordinates at the point O', such that x', y', z' are parallel respectively to x, y, z. Let r, β be the polar coordinates in the yz-plane of the point O' on the surface of the body. Let n be a unit vector which is normal to the surface element dS and positive in the inward direction. Let t be a unit vector which is tangent to the element dS, forming an angle θ with the positive x'-axis.

Let b denote a unit vector which together with n and t forms a right-handed coordinate system, such that $b = n \times t$. For a body of revolution, which is the only case to be considered here, t is tangent to a meridian and therefore lies in the plane formed by the line $O'x'$ and Ox, and b is a tangent to a circular parallel and therefore lies in the $y'z'$-plane. The angular position of the point O' (and the vector n) is given by the angle β, which is measured positive counterclockwise from the positive y'-axis. The angle θ between $O'x'$ and t is considered positive in the

sense of a counterclockwise rotation about $\mathbf{b}$.

The relations between the n, t, b-coordinate system and the x', y', z'-system (Fig.4) are given by the following table of direction cosines.

Table 1

DIRECTION COSINES

	x'	y'	z'
$\mathbf{t}$	$\cos\theta$	$\sin\theta\cos\beta$	$\sin\theta\sin\beta$
$\mathbf{b}$	0	$-\sin\beta$	$\cos\beta$
$\mathbf{n}$	$\sin\theta$	$-\cos\theta\cos\beta$	$-\cos\theta\sin\beta$
$\mathbf{V}_0$	$\cos\alpha$	0	$\sin\alpha$

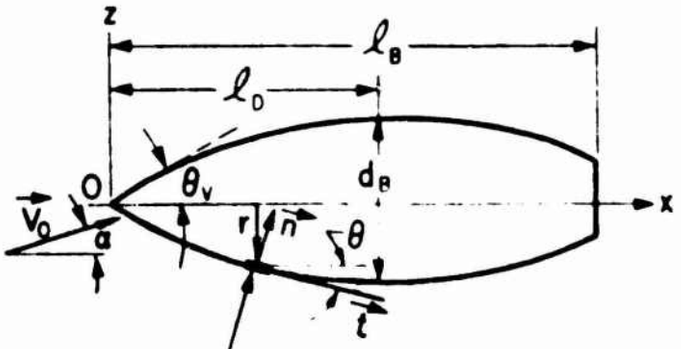

ELEMENT OF SURFACE dS

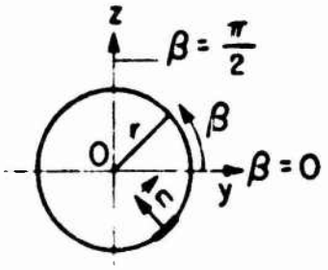

TRANSVERSE SECTION (VIEWED FROM STERN)
r = RADIUS VECTOR IN yz-PLANE TO A POINT ON THE SURFACE

V_0 = FREE-STREAM VELOCITY VECTOR

n = UNIT VECTOR NORMAL TO A SURFACE ELEMENT

t = UNIT VECTOR TANGENT TO SURFACE ELEMENT AND LYING IN A PLANE CONTAINING THE x-AXIS

d_B = MAXIMUM DIAMETER OF BODY

ℓ_B = TOTAL LENGTH OF BODY

ℓ_D = LENGTH OF DIVERGING PORTION OF BODY

θ_v = SEMI-VERTEX ANGLE AT THE NOSE

BODY OF REVOLUTION INCLINED AT AN ANGLE TO NEWTONIAN FLOW

FIG. 3

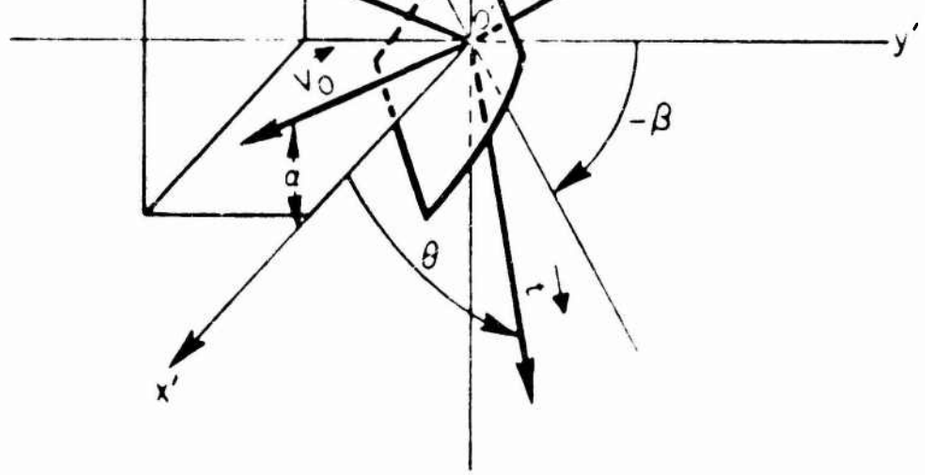

DIAGRAM OF DIRECTIONS AND COMPONENTS AT A LOCAL ELEMENT OF SURFACE AREA

FIG. 4

The free-stream velocity vector V_0 lies in the $x'z'$ -plane and makes an angle α (angle of attack) with the positive x' -axis. The angle η between the velocity vector V_0 and the normal n is given by

$$\cos \eta \equiv \cos (V_0, n) = \cos \alpha \sin \theta - \sin \alpha \cos \theta \sin \beta. \tag{3}$$

The condition for Newtonian flow is imposed by specifying that the gas stream upon striking the surface loses all of its momentum in the direction normal to the surface. Since the component of V_0 normal to the surface element dS is $V_0 \cos\eta$ and the rate of mass flow striking the element is $\rho_0 V_0 \cos\eta dS$, the rate of change of momentum on the surface element in the direction of its normal is

$$V_0 \cos \eta \times \rho_0 V_0 \cos \eta dS = \rho_0 V_0^2 \cos^2 \eta dS.$$

Thus, the excess local pressure force df produced by the momentum change is

$$df \equiv (p - p_0) dS = \rho_0 V_0^2 \cos^2 \eta dS = 2 q_0 \cos^2 \eta dS, \tag{4}$$

and the local pressure coefficient is

$$C_p \equiv \frac{p - p_0}{q_0} = 2 \cos^2 \eta = 2(\cos \alpha \sin \theta - \sin \alpha \cos \theta \sin \beta)^2. \tag{5}$$

With respect to body axes, the forces on the body may be separated into a normal force N in the z -direction and an axial force X in the x -direction, Fig. 3. For an element of area which "sees" the flow, the force components are

$$dN = -q_0 C_p \sin \beta \cos \theta \, dS = -q_0 C_p r \sin \beta \, d\beta \, dx. \tag{6}$$

since $dS \cos \theta = r \, d\beta \, dx$, and

$$dX = q_0 C_p \sin \theta \, dS = q_0 C_p r \tan \theta \, d\beta \, dx. \tag{7}$$

The total force is obtained by integration over the surface of the body. In general

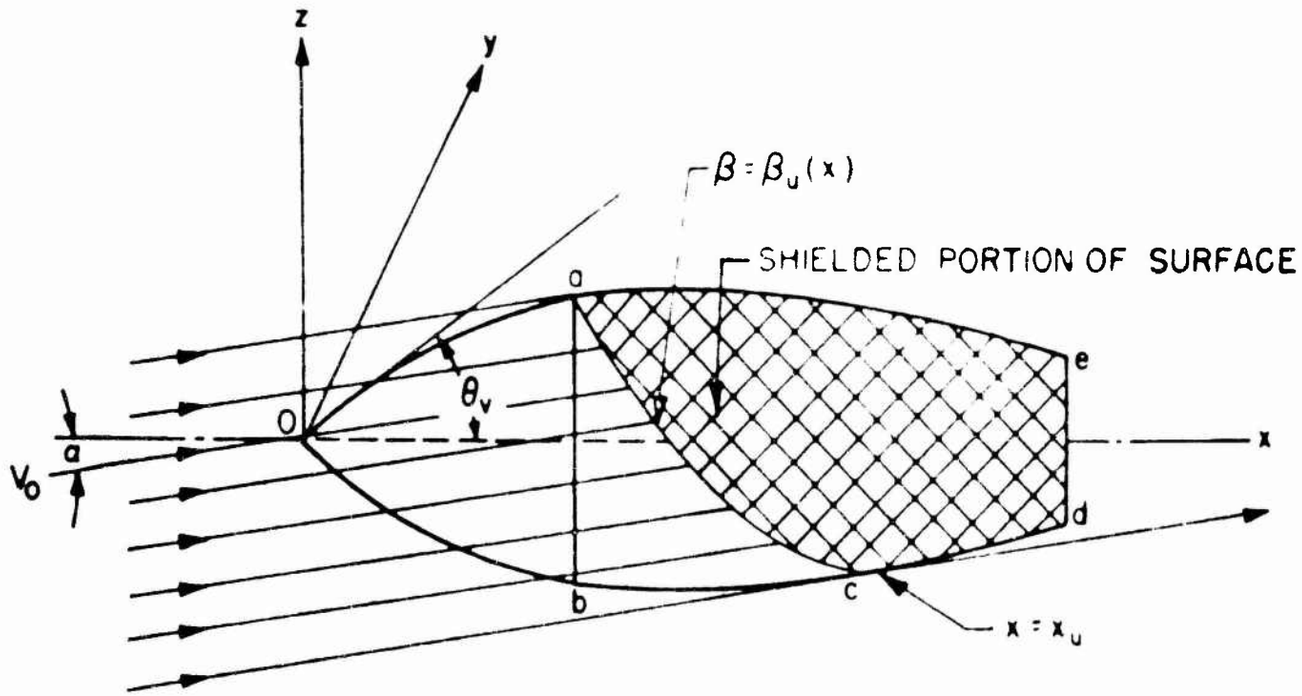

DIAGRAM TO ILLUSTRATE SHIELDED PORTION OF BODY IN NEWTONIAN FLOW

FIG.5

P-87-5

C_p will be a function of both x and β.

Consideration must now be given to those portions of the body surface which are inclined away from the free-stream direction V_0, and which may therefore be thought of as lying in the "shadow" of the free stream. This situation is illustrated in Fig. 5. As the flow proceeds over the body there will exist a boundary ac determined by the condition $C_p = 0$ (that is, $p = p_0$). All of the body surface situated upstream from ac is exposed to the oncoming flow which, upon striking the surface, undergoes compression according to Eq. (5). All of the body surface downstream from ac is in a region of expansion flow for which Eq. (5) has no meaning. Along the boundary ac the tangent vector t and the free-stream vector V_0 both lie in the same plane, the tangent plane, and consequently n and V_0 are perpendicular. This condition defines ac, and, from Eq. (3), leads to the relation

$$\cos \eta_u = \cos \alpha \sin \theta - \sin \alpha \cos \theta \sin \beta_u = 0,$$

or

$$\sin \beta_u \frac{\tan \theta}{\tan \alpha}, \tag{8}$$

where the subscript $(\ )_u$ refers to conditions along the boundary ac which defines the limit of the compression flow area.

For all transverse sections (sections normal to the x-axis) from the nose back to the section ab, the limits of integration for β are from $-\pi/2$ to $+\pi/2$. Downstream from the section ab the upper limit for β, β_u, must correspond to the points lying on the boundary ac and will be a function of x. The point c, designated by $x = x_u$, is the last point on the body to intercept any of the free-stream flow, and at this point $\beta_u = -\pi/2$ —see Fig. 5. The extreme forward tip of

(3) if $x_1, x_2, x_3, \ldots, x_{n-1}$ are in S_n,
and $x_1 + x_2 + \ldots + x_{n-1} \leq 1$, then
$f_1(x_1) + f_2(x_2) = f_1(x_2) + f_2(x_1)$.

From (3), by replacing $x_2, x_3, \ldots, x_{n-1}$ by -1, and x_1 by x, we obtain:

(4) if x is in S_n, and $x-(n-2) \leq 1$,
then $f_1(x) + f_2(-1) = f_1(-1) + f_2(x)$.

Since $x \in S_n$ implies that $x-(n-2) \leq 1$, and since, by condition (A) of the hypothesis, $f_1(-1) = f_2(-1) = -1$, we conclude from (4) that, if x is in S_n, then $f_1(x) = f_2(x)$: that is to say, that the functions f_1 and f_2 are identical. In similar fashion we see that f_i and f_j are identical, for all i and j. To simplify the notation, we set $f = f_i = f_j$. We wish to show that, for every x in S_n, $f(x) = x$.

Denote the interval

$$-1 \leq x \leq 1$$

by S. We shall show first that the conclusion of our lemma holds for every x in S. First, since 0 is in S_n, we conclude that

(5) $$f(0) = 0.$$

Now if x is any point of S, then -x is a point of S, and of course $x + -x = 0$; thus, making use of (5), we see that, for every x in S,

(6) $$f(-x) = -f(x).$$

Now from (5) and (6) and condition (B) of the hypothesis, we see that, if x, y, and $x + y$ are all in S, then

$$f(x + y) = f(x) + f(y).$$

Thus the hypothesis of Lemma 2.6 is satisfied, so we conclude that there exists a

a pointed body may be assumed to be conical over a short distance. Let the semi-vertex angle of the cone tip be denoted by θ_v . When $\alpha < \theta_v$, the point a is situated along the top meridian ($\beta = \pi/2$) at the point where $\theta = \alpha$. When $\alpha \geq \theta_v$, the point a is situated at the beginning of the body ($x = 0$). Thus, in integrating Eqs. (6) and (7) two cases must be distinguished: (1) $\alpha \leq \theta_v$, some transverse sections are completely exposed to the flow with $\beta_a = \pi/2$; (2) $\alpha > \theta_v$, the transverse sections are only partially exposed to the flow with $\beta_a = \sin^{-1}(\tan \theta / \tan \alpha)$.

Concerning the pressures on the shadowed or shielded portions of surface lying in expansion flow, which may be denoted by p_e , little can be said except that $0 < p_e < p_0$. If it should be assumed that the flow is completely separated over the shielded regions, it would then be appropriate to use $p_e = p_0$, which gives $C_{p_e} = 0$ for the pressure coefficient. The general relation for the pressure coefficient is †

$$C_{p_e} = \frac{2}{\gamma M_0^2} \left(\frac{p_e}{p_0} - 1 \right). \tag{9}$$

If it is assumed that separation does not occur, p_e / p_0 becomes very small compared to unity as M_0 increases, and when $M_0 = \infty$, both p_e / p_0 and C_{p_e} are zero. Since $C_{p_e} = 0$ for either of these possible extremes, the shielded portions of the surface would contribute nothing to the integrals of Eqs. (6) and (7).

Thus, for true Newtonian conditions corresponding to $M_0 = \infty$, the total normal and axial force on the body obtained from (6) and (7) are*

$$N = -2q_0 \int_0^{x_a} \int_{-\frac{\pi}{2}}^{\beta_a} C_p r \sin \theta \, d\beta \, dx, \tag{10}$$

and

$$\lambda = 2q_0 \int_0^{x_a} \int_{-\frac{\pi}{2}}^{\beta_a} C_p r \tan \theta \, d\beta \, dx, \tag{11}$$

†The value $\gamma = 1.4$ should be used for expansion flow.
*Although no mention has been made of the base pressure coefficient, when $M_0 = \infty$ it vanishes in the same fashion as C_{p_e} .

where C_p is given by Eq. (5). The Newtonian results (10) and (11) can be used as hypersonic approximations provided the Mach number is sufficiently large -- $M_0 = 15$, for example. When separation does not occur, C_{p_e} increases with decreasing Mach number, and as lower Mach numbers are considered ($M_0 < 10$ or 15, for example) it would be necessary to allow for values of C_{p_e} different from zero because the pressures on the expansion areas begin to have an appreciable effect on the lift. On the other hand, for decreasing Mach numbers the value of C_p given by Eq. (5) for the pressure on compression areas is less than the gas dynamic value and can therefore still be used as a conservative estimate for the compression flow. In this Mach number range an approximation to the aerodynamic forces could be written in the form

$$N = -2q_0 \int_0^{x_*} \int_{-\frac{\pi}{2}}^{\beta_*} C_p r \sin\beta \, d\beta \, dx - 2q_0 \int_0^{l_B} \int_{\beta_*}^{\frac{\pi}{2}} C_{p_e} r \sin\beta \, d\beta \, dx, \tag{12}$$

$$X = 2q_0 \int_0^{x_*} \int_{-\frac{\pi}{2}}^{\beta_*} C_p r \tan\theta \, d\beta \, dx + 2q_0 \int_0^{l_B} \int_{\beta_*}^{\frac{\pi}{2}} C_{p_e} r \tan\theta \, d\beta \, dx, \tag{13}$$

where it is understood that C_{p_e} may be put equal to zero without introducing appreciable error when the Mach number is high enough, or when separation occurs.

Before obtaining the integrals (10) and (11) for a particular body shape, it is convenient to derive the general expressions for the local forces on a transverse section. The normal force coefficient C_N for the entire body is defined by $C_N = N/q_0 \pi r_B^2$, where $d_B = 2r_B$ is the maximum diameter of the body. Axial distance along the x-axis will be expressed in units of x/d_B. Considering only the first term in (10) corresponding to the surfaces in compression flow, the local normal force coefficient per unit length, C_N', is

$$C_N' \equiv \frac{dC_N}{d\left(\frac{x}{d_B}\right)} = \frac{1}{q_0 \pi r_B^2} \frac{dN}{d\left(\frac{x}{d_B}\right)} = -\frac{4}{\pi} \frac{r}{r_B} \int_{-\frac{\pi}{2}}^{\beta_*} C_p \sin\beta \, d\beta, \tag{14}$$

where r is a function of x only. Introducing $C_p = 2(\cos\alpha\sin\theta - \sin\alpha\cos\theta\sin\beta)^2$ from (5), the integration yields

$$C'_N = \frac{4}{\pi}\frac{r}{r_B}\left\{\frac{1}{2}\left(\beta_u + \frac{\pi}{2}\right)\sin 2\alpha \sin 2\theta + \cos\beta_u\left[2\cos^2\alpha\sin^2\theta - \frac{1}{2}\sin 2\alpha \sin 2\theta \sin\beta_u + \frac{2}{3}\sin^2\alpha\cos^2\theta(\sin^2\beta_u + 2)\right]\right\}. \tag{15}$$

Introducing an axial force coefficient $C_X = X/q_0\pi r_B^2$, the local axial force coefficient per unit length is written

$$C'_X = \frac{dC_X}{d\left(\frac{x}{d_B}\right)} = \frac{1}{q_0\pi r_B^2}\frac{dX}{d\left(\frac{x}{d_B}\right)} = \frac{4}{\pi}\frac{r}{r_B}\tan\theta\int_{\frac{\pi}{2}}^{\beta_u} C_p\, d\beta, \tag{16}$$

where θ is a function of x only. The integration yields

$$C'_X = \frac{4}{\pi}\frac{r}{r_B}\tan\theta\left[\left(\beta_u + \frac{\pi}{2}\right)(2\cos^2\alpha\sin^2\theta + \sin^2\alpha\cos^2\theta) + \cos\beta_u(\sin 2\alpha\cos 2\theta - \sin^2\alpha\cos^2\theta\sin\beta_u)\right]. \tag{17}$$

Distinction is now made between the two cases $\alpha \le \theta_v$, and $\alpha > \theta_v$.

Case 1. $\alpha \le \theta_v$

For this case $\beta = \pi/2$ and Eqs. (15) and (17) reduce to

$$C'_N = 2\frac{r}{r_B}\sin 2\alpha \sin 2\theta \tag{18}$$

and

$$C'_X = 4\frac{r}{r_B}\tan\theta[2\sin^2\theta + \sin^2\alpha(1 - 3\sin^2\theta)]. \tag{19}$$

Case 2. $\alpha > \theta_v$

In this case, Eq. (8),

$$\beta_u = \sin^{-1}\left(\frac{\tan\theta}{\tan\alpha}\right)$$

and

$$\cos\beta_u = \sqrt{1 - \frac{\tan^2\theta}{\tan^2\alpha}},$$

and Eqs. (15) and (17) reduce to

$$C'_N = 4\frac{r}{r_B}\cos^2\theta\sin 2\alpha\left[\frac{\left(\beta_u + \frac{\pi}{2}\right)}{\pi}\tan\theta + \frac{1}{3\pi}\cos\beta_u(\cot\alpha\tan^2\theta + 2\tan\alpha)\right], \tag{20}$$

$$C'_X = 4\frac{r}{r_B}\tan\theta\left[\frac{\left(\beta_u + \frac{\pi}{2}\right)}{\pi}[2\sin^2\theta + \sin^2\alpha(1 - 3\sin^2\theta)] + \frac{3}{4\pi}\cos\beta_u\sin 2\alpha\sin 2\theta\right]. \tag{21}$$

Equations (18) through (21) are the general expressions for the normal and axial forces on local transverse sections of the body, assuming $C_{p_s} = 0$ on the shielded surfaces and neglecting centrifugal forces in the flow. The total normal and axial forces are obtained by integrating these local values over the length of the body. In order to apply the equations to a particular body of revolution, the profile of the body shape is introduced by specifying θ as a function of x. Of particular interest in missile aerodynamics is the body consisting of cone plus cylinder. According to the Newtonian approximation which has been outlined, the pressure forces on a body are determined entirely by the local value of θ; consequently, the force on any portion of a body may be evaluated separately, and the total force obtained by addition.

B. CONE

For a right circular cone of length ℓ_D, base radius r_D and semi-vertex angle θ_v, we have

$$x_u = \ell_D = \frac{r_D}{\tan \theta_v}, \qquad \theta = \text{const} = \theta_v, \qquad \frac{r}{r_B} \equiv \frac{r}{r_D} = \frac{x}{\ell_D}.$$

As before two cases must be distinguished corresponding to $\alpha \leq \theta_v$, and $\alpha > \theta_v$.

Case 1. $\alpha \leq \theta_v - \beta_u = \pi/2$.

From (18) it follows that

$$C_N = \int_0^{\frac{\ell_D}{d_D}} C_N' \, d\left(\frac{x}{d_D}\right) = \frac{\ell_D}{d_D} \sin 2\theta_v \sin 2\alpha.$$

Since $\ell_D/d_D = 1/(2 \tan \theta_v)$, this may be written

$$C_N = \cos^2 \theta_v \sin 2\alpha. \tag{22}$$

Similarly, from (19) the axial coefficient is

$$C_X = 2 \sin^2 \theta_v + \sin^2 \alpha (1 - 3 \sin^2 \theta_v). \tag{23}$$

It is interesting to examine the value of the initial lift curve slope for the cone. It is simply

$$\left(\frac{dC_L}{d\alpha}\right)_{\alpha=0} \equiv \left(\frac{dC_N}{d\alpha}\right)_{\alpha=0} = 2\cos^2\theta_v. \tag{24}$$

For a very slender cone ($\theta_v \to 0$) this reduces to the slender body result, $dC_L/d\alpha = 2$. This gives the rather surprising result that at small angles of attack the lift coefficient for a slender diverging body has very nearly the same value at very high Mach numbers as at very low supersonic speeds. This indicates that for a body of this type at small angles of attack the lift coefficient is essentially independent of Mach number. This conclusion is completely borne out by the Stone-Kopal values for cone lift at small angle of attack shown in Fig. 1.

Case 2. $\alpha > \theta_v - \beta_u = \sin^{-1}(\tan\theta_v/\tan\alpha)$.

For this case it follows from (20) that

$$C_N = \cos^2\theta_v \sin 2\alpha\left[\frac{\left(\beta_u + \frac{\pi}{2}\right)}{\pi} + \frac{1}{3\pi}\cos\beta_u(\tan\theta_v \cot\alpha + 2\cot\theta_v \tan\alpha)\right], \tag{25}$$

and from (21) that

$$C_X = \frac{\left(\beta_u + \frac{\pi}{2}\right)}{\pi}\left[2\sin^2\theta_v + \sin^2\alpha(1 - 3\sin^2\theta_v)\right]$$

$$+ \frac{3}{4\pi}\cos\beta_u \sin 2\theta_v \sin 2\alpha. \tag{26}$$

The center of pressure on the cone may be found by taking moments about the vertex. If a is the distance from the vertex to the center of pressure, this distance is determined by the relation

$$a = \frac{\text{moment}}{\text{normal force}} = \frac{d_D\int_0^{\frac{x}{d_D}=\frac{\ell_D}{d_D}} \frac{x}{d_D} C_N' \, d\left(\frac{x}{d_D}\right)}{C_N}. \tag{27}$$

Using either (22) or (25), it is found that

$$a = \tfrac{2}{3}\ell_D. \tag{28}$$

C. CYLINDER.

To determine the Newtonian pressures on a circular cylinder, consider an infinite circular cylinder in a flow which is inclined at an angle α to the longitudinal axis of the cylinder. In the case of a circular cylinder it is evident that only the lower half of the cylindrical surface is exposed to the free-stream (case 2) and therefore that $\beta_s = 0$. Also, since $\theta = 0$ and $r = r_B = \text{const} = r_S$ (the subscript S is used to denote cylinder) for a circular cylinder, it follows from (20) that

$$C_N' = \frac{16}{3\pi} \sin^2 \alpha. \tag{29}$$

If ℓ_S is used to denote the length of any portion of the infinite cylinder, the normal force coefficient is

$$C_N \equiv \frac{N}{q_0 \pi r_S} = \frac{16}{3\pi} \frac{\ell_S}{d_S} \sin^2 \alpha = \frac{5.33}{\pi} \frac{\ell_S}{d_S} \sin^2 \alpha, \tag{30}$$

where N is the normal force on the cylinder length ℓ_S . The axial force on the cylinder of course is zero. Also $(dC_N'/d\alpha)_{\alpha=0}$ is zero.

When the effect of centrifugal forces as influenced by the boundary layer is considered in addition to the impact (Newtonian) forces, the normal force on the cylinder is reduced by ten percent (see Appendix). Thus (29) and (30) become

$$C_N' = \frac{4.8}{\pi} \sin^2 \alpha \tag{31}$$

and

$$C_N = \frac{4.8}{\pi} \frac{\ell_S}{d_S} \sin^2 \alpha. \tag{32}$$

The analysis including centrifugal forces indicates that such effects are smaller for conventional slender noses such as cones and ogives at moderate angles of attack and thus the pressure forces on such slender noses are satisfactorily approximated by the Newtonian (impact force) method. Consequently, the aerodynamic characteristics of a cone as given by equations (27) through (28) are not modified.

D. THE CONE AND CYLINDER AREAS SITUATED IN EXPANSION FLOW.

All of the expressions (14) through (32) can be interpreted in two ways. For truly Newtonian conditions corresponding to $M_0 = \infty$, it was pointed out previously that $C_{p_e} = 0$ and $p_e/p_0 = 0$. In this case the formulas (14) through (30) give the total forces on the entire body, including the surfaces situated in expansion flow. If the formulas (14) through (30) are considered as hypersonic approximations, they may be thought of as applying only to the forces on the surfaces in compression flow. In this case—as discussed in connection with Eqs. (12) and (13)—it is appropriate to consider a non-zero value for the pressure coefficient C_{p_e} where

$$C_{p_e} = \frac{2}{\gamma M_0^2}\left(\frac{p_e}{p_0} - 1\right),$$

corresponding to the surface areas situated in expansion flow. Although C_{p_e} is certainly negligible at very high Mach numbers, it would have to be given consideration in any attempt to extrapolate the hypersonic approximations down to lower Mach numbers. In view of the extremely approximate nature of such a procedure, it would probably be sufficient to use an average value $\bar{p}_e$ which is independent of β but which may be different on the cone and on the cylinder.

1. Cone

If an average pressure is used, from Eq. (12) the normal force N_e on the expansion flow areas of the cone would be written

$$N_e = \frac{4q_0}{\gamma M_0^2}\left(1 - \frac{\bar{p}_{e_D}}{p_0}\right)\int_0^{\ell_D}\int_{\beta}^{\frac{\pi}{2}} r \sin\beta \, d\beta \, dx,$$

where $\bar{p}_{e_D}$ is the average pressure on the shielded area of the cone, and $\beta = \sin^{-1}(\tan\theta_v/\tan\alpha)$. The corresponding normal force coefficient C_{N_e} is

$$C_{N_e} = \frac{N_e}{q_0 \pi r_D^2} = \frac{2\left(1 - \frac{\bar{p}_{e_D}}{p_0}\right)}{\pi\gamma M_0^2}\sqrt{\cot^2\theta_v - \cot^2\alpha}. \qquad (33)$$

Similarly, the axial coefficient is found to be

$$C_{X_e} = -\frac{2\left(\frac{\bar{p}_{e_D}}{p_0} - 1\right)}{\pi\gamma M_0^2}\left(\frac{\pi}{2} - \beta_a\right). \tag{34}$$

2. Cylinder

For the cylinder, since $\beta_a = 0$, r = const, and it is assumed that $p = \bar{p}_e$ = const, the result is

$$C_{N_e} = \frac{q_0 C_{p_e} \ell_s d_s}{q_0 \pi r_s^2} = \frac{4\,\ell_s}{\pi\, r_s}\,\frac{\left(\frac{\bar{p}_{e_S}}{p_0} - 1\right)}{\gamma M_0^2}. \tag{35}$$

In order to use these equations approximate values for $\bar{p}_{e_D}$ and $\bar{p}_{e_S}$ must be estimated in any manner which appears feasible, possibly from two-dimensional gas dynamics and low aspect ratio supersonic wing theory. An indication of the maximum effect of the expansion pressures on the lift of a yawed body is obtained by putting $\bar{p}_{e_D} = \bar{p}_{e_S} = 0$. This is shown in Fig. 7 for a typical body. The actual lift (normal force) could be expected to be somewhere between the two curves shown in Fig. 6.

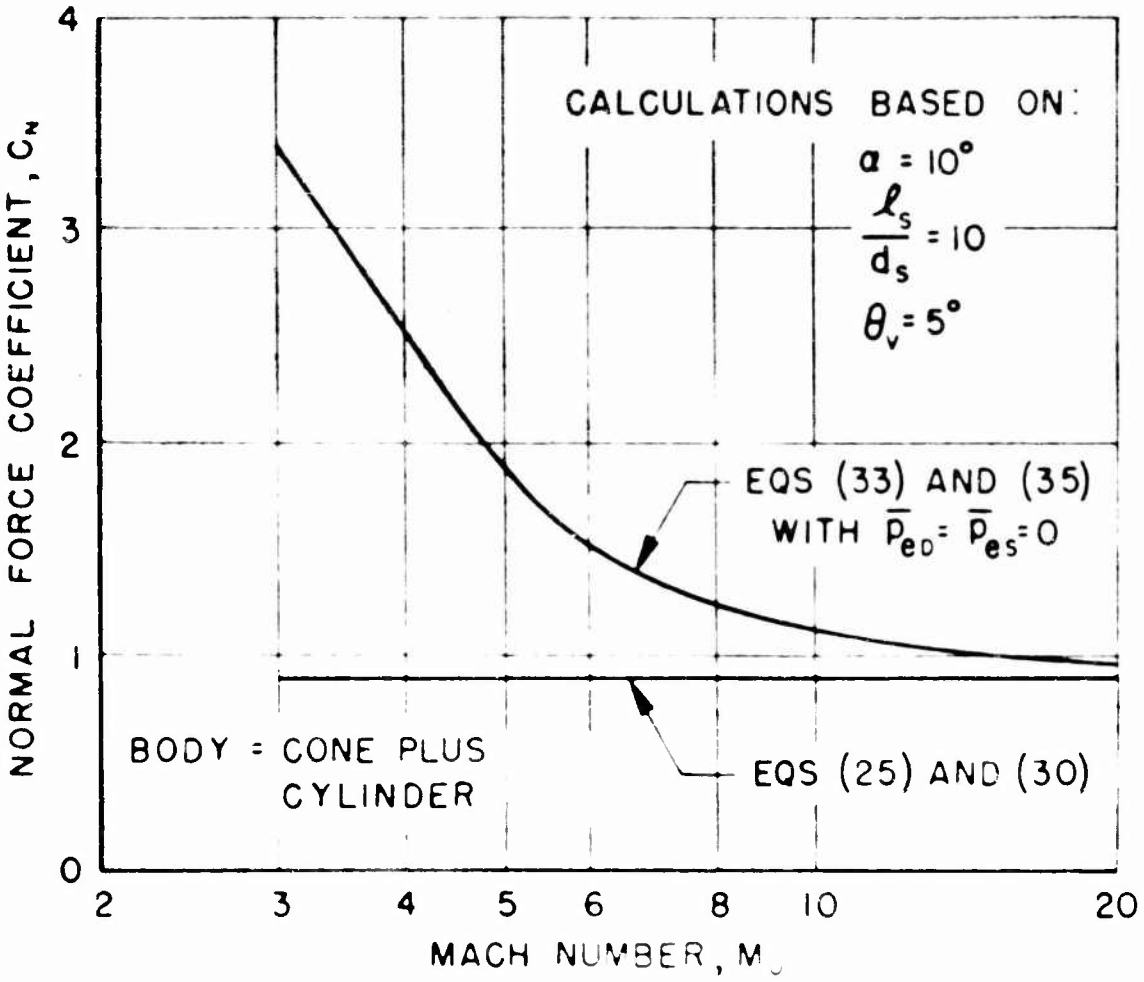

ILLUSTRATION OF LOW MACH NUMBER EFFECT OF EXPANSION FLOW ON THE LIFT OF A YAWED BODY OF REVOLUTION

FIG. 6

15-a

III. THE CORRELATION OF EXPERIMENTAL RESULTS FOR THE SUPERSONIC LIFT ON BODIES OF REVOLUTION

The previous discussions have been concerned entirely with approximate methods for predicting the lift of a body of revolution at hypersonic Mach numbers, of the order of 10 or 15 and above. Since it is important to have values of body lift throughout the complete Mach number range, this still leaves the problem of estimating body lift at all lower Mach numbers. Because of the lack of theoretical results applicable to this range of Mach number ($2 < M_0 < 10$), a study has been made of available experimental data and an attempt made to use the indications of these results to estimate (interpolate) the body lift in the intermediate range of Mach number. For this purpose use is made of the hypersonic approximation for the upper end of the Mach number range. This procedure is admittedly almost qualitative in some respects, and it is expected that at least some of the results given here will have to be modified as more theoretical and experimental data become available.

The amount of available systematic supersonic experimental data for yawed bodies of revolution appears to be extremely limited. A survey of all supersonic data on yawed bodies of revolution shows that there exists no complete systematic series of tests (at least with data in usable form) in which body lift is determined as a function of angle of attack, Mach number, and body fineness ratio—particularly for varying lengths of cylinder behind the same nose shape. Except for the very complete tests on the A4[7] and the Wasserfall,[8] there is a great scarcity of pressure distribution data for yawed bodies. This type of information is quite essential if significant comparisons are to be made with any theoretical results. Even for so simple a shape as a cone there are but very fragmentary pressure distribution data for the yawed condition.[9] Moreover, most of the systematic experimental work in the past has been limited to body fineness ratios (l_B/d_B) of 7 or less.[10] The

importance of tests on bodies of large fineness ratio lies in the indications of the discussion below that the lift on the cylindrical part of the body behind the nose not only becomes appreciable, Fig. 7, but also—at high enough speeds, Eq. (32)—the lift is directly proportional to the cylinder length and to the square of the angle of attack. While much is to be desired by way of experimental data, by using the hypersonic approximation as a guide together with available experimental results, it has been possible to obtain a rather consistent correlation for body lift over a wide range of conditions.

A. LIFT ON A CYLINDER FOLLOWING A CONE OR OGIVE

From the close agreement in Fig. 1 between the hypersonic approximation and the Stone-Kopal values for cone lift, it is evident that the hypersonic-approximation values give a good approximation for cone lift even at low supersonic Mach numbers. It is instructive to compare, at low Mach numbers, the hypersonic approximation for cylinder lift with the experimental values for the lift on a cylinder following a cone or ogive. It is possible to extract some rather definite indications in this regard from the very complete pressure distribution data for the German A4 missile at angle of attack.[7] The A4 body has an ogival nose followed by a straight cylindrical section which extends back to the beginning of the tail surfaces, beyond which there is a boattail. If x is the distance measured from the forward tip of the nose and d_B denotes the maximum body diameter ($d_B = d_S$, the diameter of the cylindrical section), the straight cylindrical section extends from x/d_B=3.5 to x/d_B= 6.0 giving a cylinder length of 2.5 calibers.

The data in Ref. 7 give the local normal force coefficients C_N' as a function of position x/d_B along the body, for a range of Mach number and angle of attack. These local values of C_N' have been integrated over the cylinder section and give the cylinder lift values shown in Fig. 7. These results show that at supersonic

speeds the cylindrical portion of a body contributes very appreciable lift—which is rather strongly dependent on angle of attack and Mach number, and emphasize the extremely poor approximation given by the slender body (0-order) theory—which predicts zero lift on the cylinder, and by the linearized (1st-order) theories which predict only very limited cylinder lift. Figure 7 also indicates that for low supersonic speeds the lift on the cylinder has already exceeded the hypersonic-approximation value and is increasing rapidly with Mach number. At high enough Mach numbers, yet to be determined, these curves must decrease to the hypersonic-approximation values. In view of the constant value of the normal force coefficient for a cone, for example, this suggests that the normal force coefficient for a cone plus cylinder body must go through a maximum with respect to Mach number. It will be seen later that this is exactly what is indicated by the analysis of available experimental data.

The qualitative notions concerning the lift distribution on a cylinder following an ogive are indicated by Fig. 8. At low supersonic Mach numbers ($M_0 = 2$ to 3) the local normal force coefficient C_N' decreases with distance downstream along the axis of the cylinder but gives and integrated lift coefficient C_N which is greater than the hypersonic-approximation value. At some higher Mach number, probably in the range $3 < M_0 < 6$, C_N reaches its highest value. At still higher Mach numbers the variation of C_N' along the cylinder axis becomes smaller and smaller, approaching a constant condition, and C_N approaches the hypersonic-approximation value. The Mach number at which the total body lift becomes approximately equal to the hypersonic-approximation value will be discussed below on the basis of the indications of the experimental data.

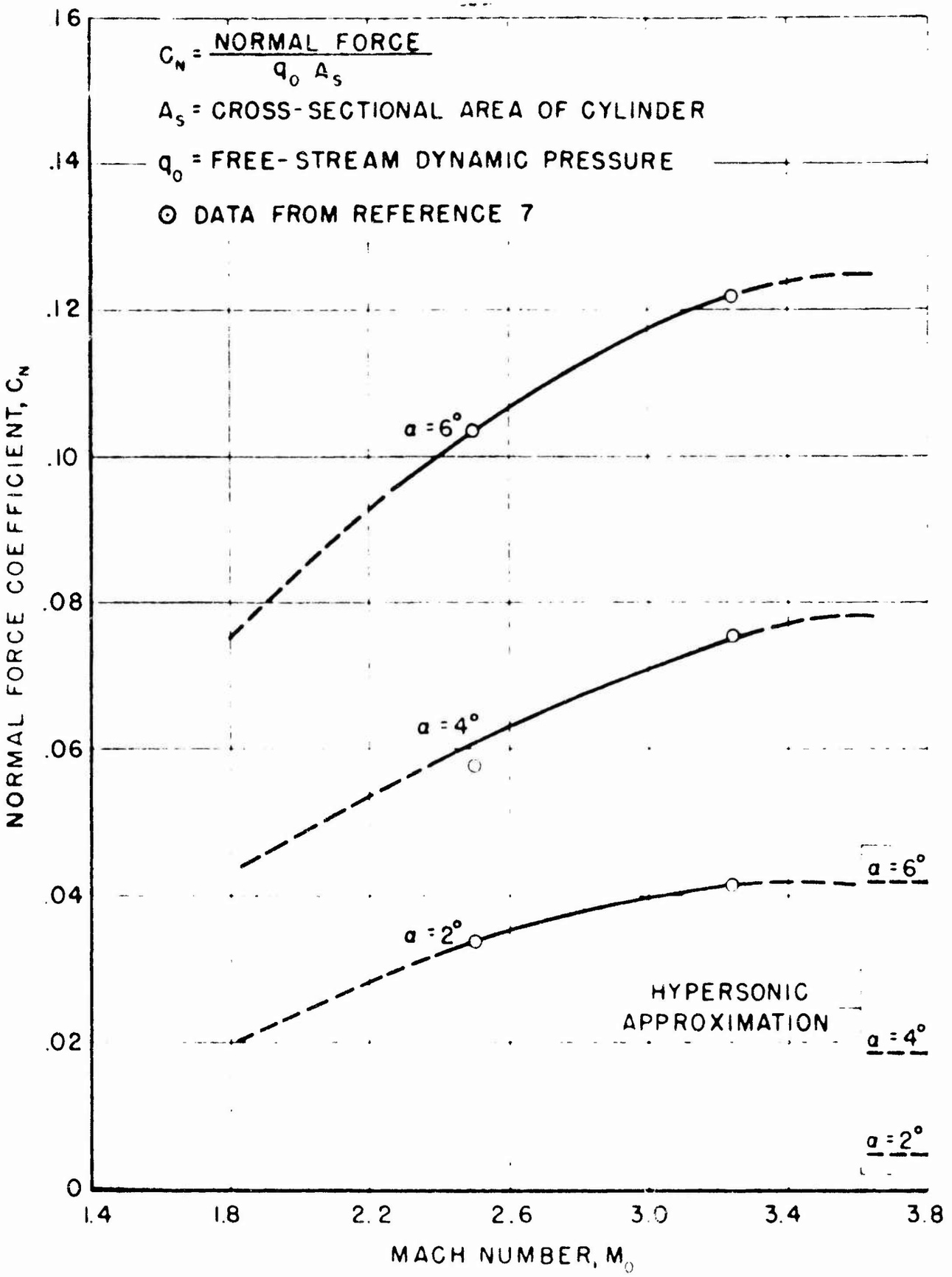

NORMAL FORCE COEFFICIENT FOR A CIRCULAR CYLINDER SITUATED BEHIND AN OGIVE — THE GERMAN A4 MISSILE

FIG. 7

P-87-15

B. THE INITIAL NORMAL FORCE SLOPE FOR MISSILES WITH CYLINDRICAL AFTERBODIES

A typical missile body is shown schematically in Fig. 9. It consists of a diverging section (nose) of length l_n, which may be either a cone or an ogive, a straight (cylindrical section) of length l_s and a converging (boattail) section of length l_c. The semi-vertex angle of the nose cone, or of the inscribed cone when the nose is ogival, is denoted by θ_n. The total body length is l_B, the maximum body diameter d_B, the maximum cross-section area $A_B = (\pi/4)\, d_B^2$, and the diameter of the base d_b. All of the body aft of the nose, or forebody, may be referred to as the afterbody, and its length denoted by $l_A (= l_s + l_c)$. The afterbody may consist of all cylinder, part cylinder and part boattail, or all boattail. In general, the variables upon which the normal force coefficient will depend may be indicated by the relation

$$C_N \equiv \frac{\text{normal force}}{q_0 A_B} = \text{func}\left(\theta_n, \frac{l_A}{d_B}, \frac{d_b}{d_B}, M_0, \alpha\right). \tag{36}$$

For the case in which the entire afterbody is cylindrical (no boattail), it follows that $l_A = l_s$, $d_B = d_s$ and the dependency of C_N becomes

$$C_N \equiv \frac{\text{normal force}}{q_0 A_B} = \text{func}\left(\theta_n, \frac{l_s}{d_s}, M_0, \alpha\right). \tag{37}$$

Since most of the available lift data are restricted to small angles of attack, such results are employed to greatest advantage when they are used to evaluate $(dC_N/d\alpha)_{\alpha=0}$. From equation (24) and Figs. 1 and 2 it appears that the normal force on the conical nose varies approximately as $\cos^2\theta_n$, and this suggests use of the parameter $\left(\frac{dC_N}{d\alpha}\right)_{\alpha=0} / \cos^2\theta_n$. However, most of the test data fall within the range $5° \leq \theta_n \leq 15°$ so the variation of $\cos^2\theta_n$ from its median value is less than 4 percent and within the accuracy of the experimental data. Furthermore, an investigation of the lift on the cylinder

37-15

immediately following a cone (using yawed cone data (2) and Prandtl-Meyer expansions) indicates that the cylinder lift may vary with cone semi-vertex angle so as to counteract the variation of cone lift with θ_v . For these reasons θ_v is eliminated and the experimental correlation is reduced to the form

$$\left(\frac{dC_N}{d\alpha}\right)_{\alpha=0} = \text{func}\left(\frac{l_s}{d_s} , M_0\right) \tag{38}$$

This correlation has been carried out and yields the results* shown in Fig. 10. While the experimental points (not indicated) show considerable scatter, the correlation is sufficiently good to define individual curves for cone and ogive nose shapes and is considered fairly satisfactory, at least for preliminary purposes. It is found that when the length of the afterbody exceeds about 3 diameters (calibers), as far as total lift is concerned it makes little difference whether the nose is an ogive or a cone. At the lower Mach numbers, the curves go through a maximum with respect to both afterbody fineness ratio and Mach number. As l_s/d_s becomes large (> 9), the initial normal force slope becomes essentially independent of afterbody length. At the higher Mach numbers, $M_0 > 9$, the initial slope becomes equal to that given by the hypersonic-approximation for a cone. This follows from the fact that a cylindrical afterbody contributes nothing to the initial normal force slope in hypersonic flow--Eq. (30). At hypersonic speeds the ogive normal force is approximately equal to the normal force on its inscribed cone, as has been assumed in Fig. 10.

$^2\theta_v$.

*It will be noted that the abscissa in Fig. 10 is labeled l_A/d_B , and therefore not limited to missiles without boattail. It is pointed out in Section D that the effect of boattail may be accounted for as an increment in initial normal force slope (see Fig. 15) which must be added to the values obtained from Fig. 10. When there is no boattail, $l_A/d_B = l_s/d_B$, and the values of Fig. 10 apply directly.

C. ADDITIONAL NORMAL FORCE RESULTING FROM ANGLE OF ATTACK

If the normal force curve slope were independent of α , the normal force could then be obtained immediately from Fig. 10. However, except for very small angles of attack and missiles with no afterbody, the normal force is found to depart widely from a linear variation with α , and to vary in a manner which is more nearly a quadratic function of α. This effect of angle of attack on normal force can be studied by introducing an increment in normal force coefficient, ΔC_N , defined by

$$C_N = \left(\frac{dC_N}{d\alpha}\right)_{\alpha=0} \times \alpha + \Delta C_N \tag{39}$$

This is illustrated in Fig. 11. Formula (39) is the relation used to correlate angle of attack conditions, including the effects of Mach number and afterbody length at angle of attack. It appears that, within the accuracy of the data, ΔC_N varies as $\sin^2\alpha$ so the results of the correlation are presented in the form $\Delta C_N/\sin^2\alpha$. Before giving the results of this correlation, it is worthwhile to point out how the hypersonic approximations may be used to extrapolate from the limited range of conditions covered by the experimental results to conditions of higher Mach number and angle of attack.

By using the experimental correlation results such as those of Figs. 10 and 11, it is possible to obtain experimentally-based estimates of C_N up to $M_0 = 4$, over a range of values of l_s/d_s and α . These are shown by the left-hand end of the curves ($M_0 \leq 4.0$) in Figs. 12 and 13. At the high Mach number end ($M_0 \approx$ 15 or 20, and higher) we have the hypersonic-approximation values which are independent of Mach number. As explained in Part II-D, by extending the hypersonic-approximation to lower Mach numbers using $p_e = 0$ for the surfaces in expansion flow, an indication is obtained of the limits within which the actual value of C_N must lie. These limits are shown as curves 1 and 2 in Fig. 12, for example. Since there is no experimental data for $M_0 > 4.31$, and most of the experimental data does not extend beyond $M_0 = 3$,

these limit curves may be used as a guide for extending the low Mach number range into the hypersonic range. This is the procedure which has been followed to obtain the results shown in Figs. 12 and 13. While this procedure admittedly contains certain elements of arbitrariness, it is believed to yield fairly realistic results and at least gives preliminary working values for lift over a range of conditions for which no other information exists.

By employing results of the type shown in Figs. 12 and 13, the correlated values of ΔC_N (Fig. 11) from test data have been extended into the hypersonic region as shown in Fig. 14. The hypersonic-approximation for cones gives C_N as practically a linear function of angle of attack for the low angle of attack range $(\alpha < 2\theta_c)$ which is of most interest. The meager experimental cone data indicate that this is also true at low supersonic speeds. Thus the additional normal force coefficient ΔC_N for a cone is zero, at least to the same degree of accuracy as can be expected from the experimental data. Consequently, it follows that the ΔC_N values in Fig. 14 refer to the cylinder only, and for $M_0 = \infty$ are given by formula (32).

D. EFFECT OF BOATTAIL

A preliminary correlation of available data have shown the effect of boattail on normal force to be limited to the initial normal force slope, $(dC_N/d\alpha)_{\alpha=0}$.

No consistent, pronounced effect on the additional normal force, ΔC_N, was found within the angle of attack range of the tests ($\alpha \leq 10°$). It is likely, however, that data at higher angles of attack ($\alpha > 10°$) would show some effect of boattail on ΔC_N. It appears that the initial normal force slope decreases linearly with decreasing base ratio, d_b/d_s, over the normal range of base ratios—$0.4 \leq d_b/d_s \leq 1.0$. The effects of boattail angle and type (conical or ogival) and the body preceding the boattail appear to be small compared with the effect of the base ratio. The

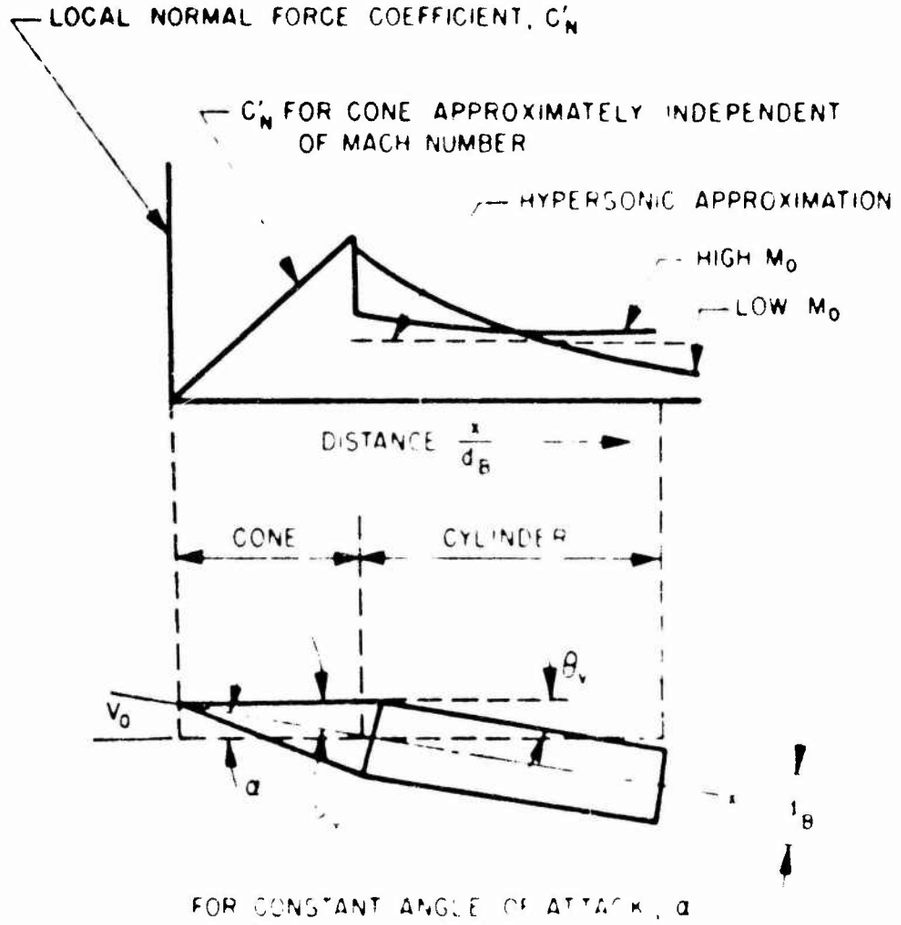

SCHEMATIC DIAGRAM TO ILLUSTRATE THE EFFECT OF INCREASING MACH NUMBER ON THE DISTRIBUTION OF C'_N ALONG A CYLINDRICAL SECTION BEHIND A CONE

FIG. 8

P-82
P-82 (a)

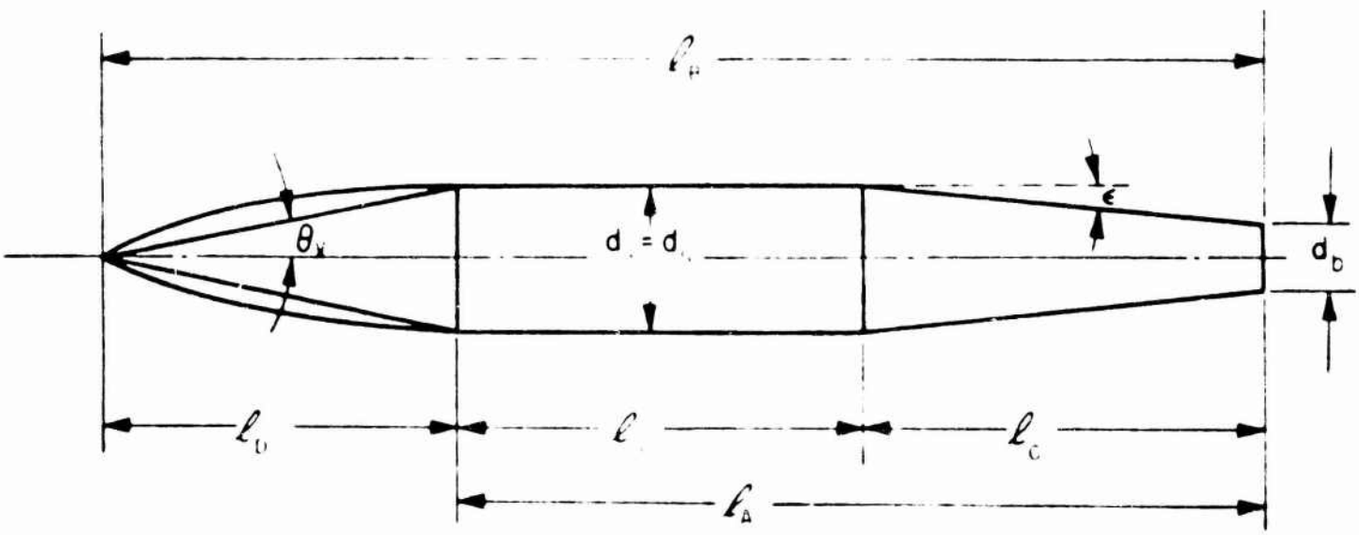

θ_v = SEMI-VERTEX ANGLE OF INSCRIBED CONE

d_B = MAXIMUM DIAMETER OF BODY

$A_B = \frac{\pi}{4} d_B^2$ = MAXIMUM CROSS SECTION AREA OF BODY

ϵ = BOATTAIL ANGLE

d_b = BASE DIAMETER

ℓ_B = TOTAL LENGTH OF BODY

ℓ_D = LENGTH OF NOSE, OR DIVERGING SECTION

ℓ_S = LENGTH OF STRAIGHT OR CYLINDRICAL SECTION

ℓ_C = LENGTH OF CONVERGING SECTION

DIAGRAM OF TYPICAL MISSILE BODY - SCHEMATIC

FIG. 9

P-87-17
P-87-17a

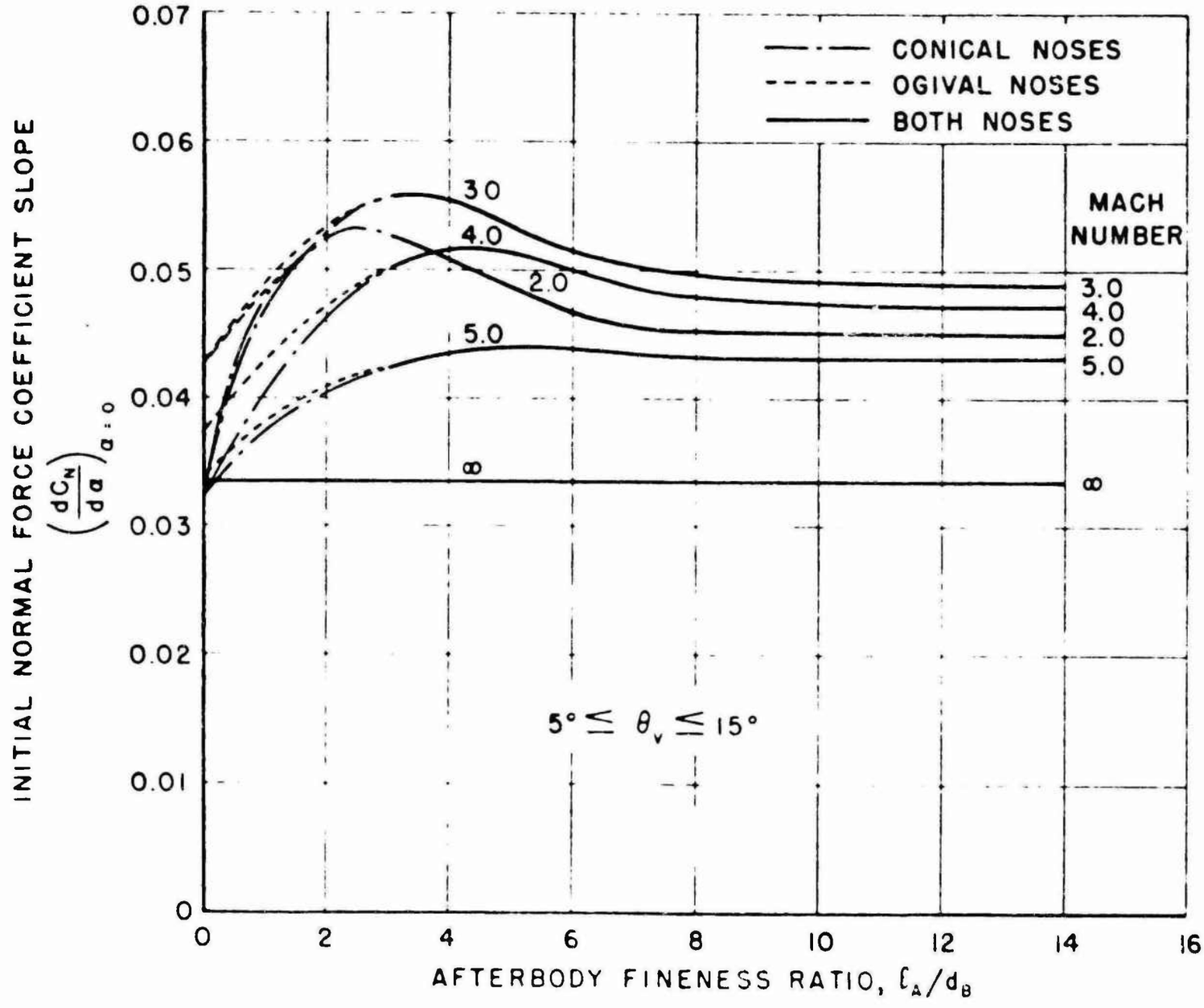

INITIAL NORMAL FORCE SLOPE FOR MISSILES WITH CYLINDRICAL AFTERBODIES

FIG. 10

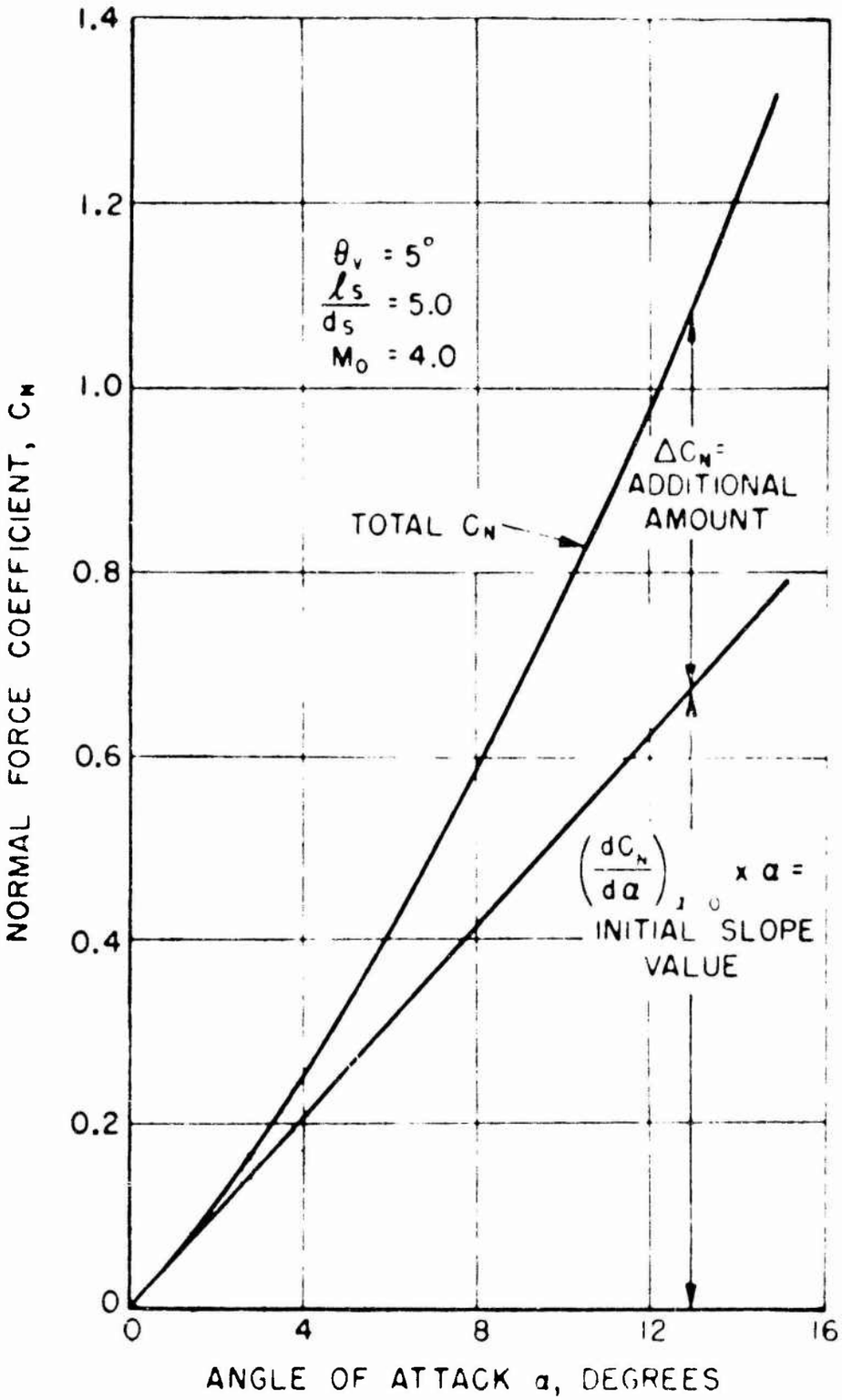

DIAGRAM TO ILLUSTRATE TYPICAL VARIATION OF NORMAL FORCE COEFFICIENT WITH ANGLE OF ATTACK-SCHEMATIC

FIG. 11

P-87-19
P-87-19a

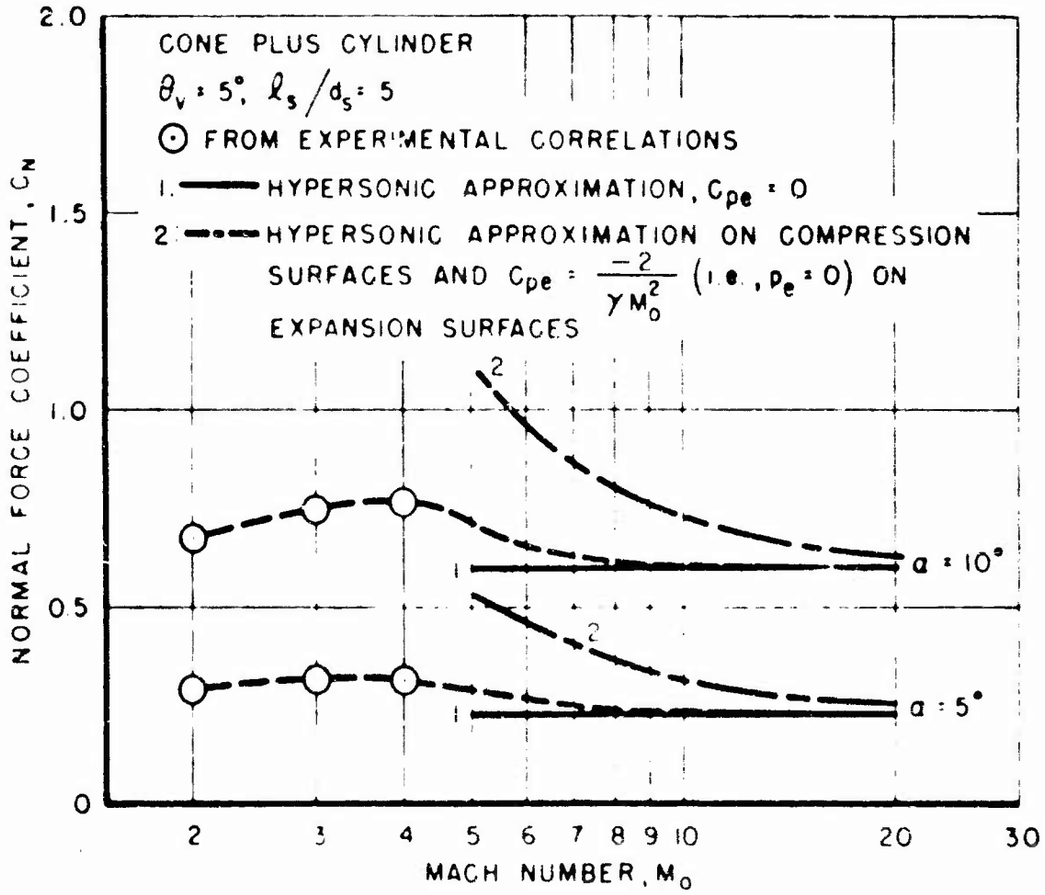

VARIATION OF NORMAL FORCE COEFFICIENT WITH MACH NUMBER AND ANGLE OF ATTACK

FIG. 12

P-87-20a

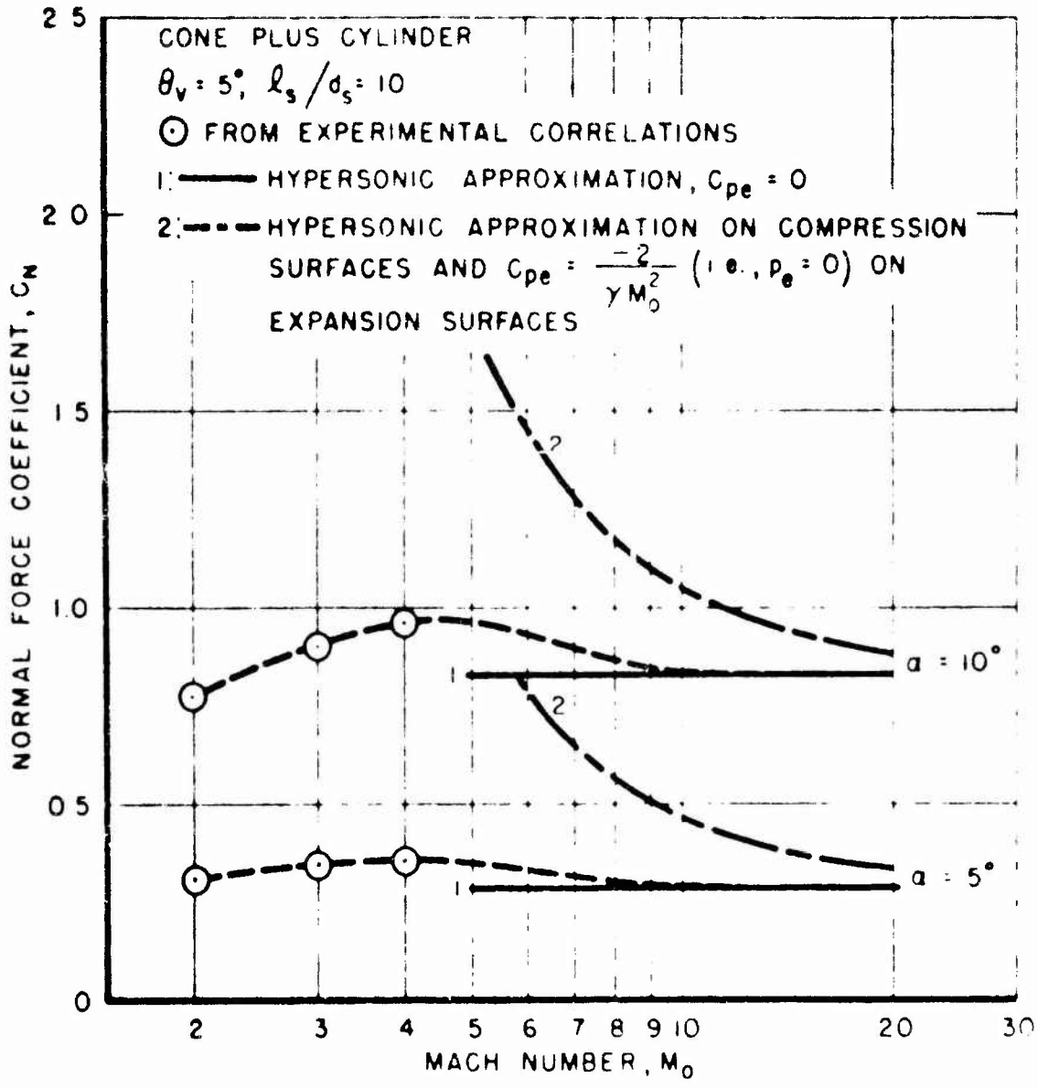

VARIATION OF NORMAL FORCE COEFFICIENT WITH MACH NUMBER AND ANGLE OF ATTACK

FIG. 13

P-87-210

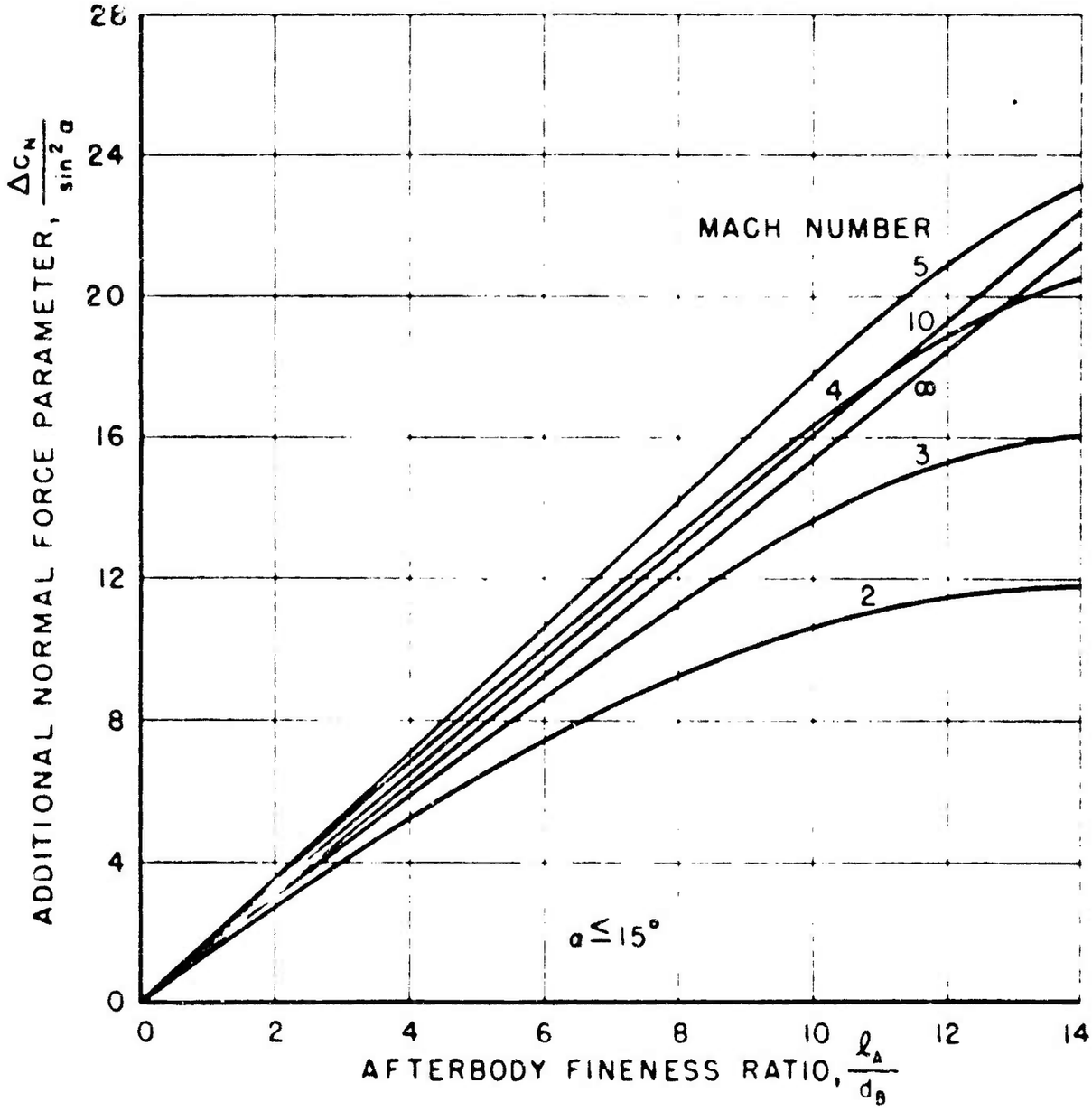

ADDITIONAL NORMAL FORCE PARAMETER

FIG. 14

P87-28a

The results of this correlation are shown by Fig. 15. It will be noted that the boattail effect is a maximum at low speeds, and decreases to zero at about $M_0 = 9$. This is in agreement with the slender-body theories [11] which predict zero lift when $d_b/d_s = 0$, and with the hypersonic-approximation which indicates no boattail effect on the initial slope parameter. It should be mentioned, however, that the hypersonic-approximation would show an effect of boattail on ΔC_N, since the boattail portion of the body would be completely shielded at angles of attack less than the boattail angle.

E. CENTER OF PRESSURE

By using the normal forces which have been estimated for any cone-cylinder or ogive-cylinder combination, it is possible to estimate the corresponding center of pressure. Figures 10 and 14 give the normal force on a cone or ogive and the normal force distribution along a cylinder following the cone or ogive. The center of pressure of the cone and ogive are approximately $0.67\ell_n$ and $0.53\ell_n$, respectively, aft of the nose. Figure 15 gives the increment in normal force due to boattail. It appears satisfactory to assume that this force acts at the mid-point of the boattail. The location of the missile center of pressure aft of the nose tip, $x_{c.p.}$, is obtained by forming the summation of the various components according to the formula

$$x_{c.p.} = \frac{\sum C_{N_b} x_b}{\sum C_{N_b}} \tag{40}$$

Preliminary checks of this method have shown satisfactory agreement with experimental data.

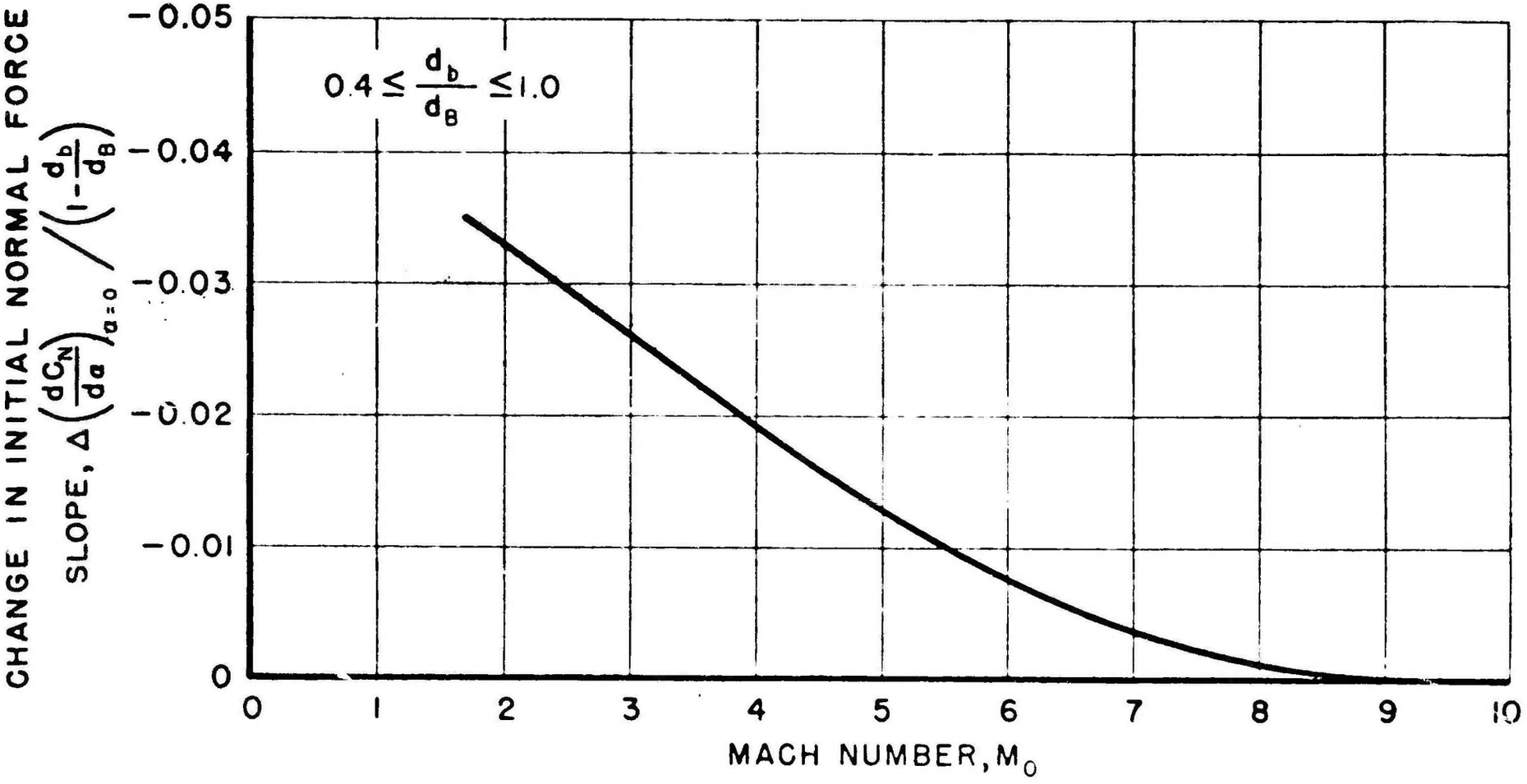

DECREASE IN INITIAL NORMAL FORCE SLOPE DUE TO BOATTAIL

FIG. 15

APPENDIX
ANALYSIS OF THE CENTRIFUGAL FORCE EFFECTS

GENERAL DISCUSSION

The simple analysis of Newtonian flow is incomplete inasmuch as the effects of centrifugal forces in the flow around the body have been neglected. In the flow over plane surfaces at angle of attack and on cones at zero angle of attack, since the paths of the air particles over such surfaces (that is, the streamlines on the surfaces) are straight lines, no centrifugal forces are present. However, when the surface streamlines are curved--as is the case for bodies of revolution at angle of attack, for example--centrifugal forces will be present in the flow. For these flow problems, the total surface pressure coefficient at any point on the body is equal to the impact pressure coefficient minus the centrifugal pressure effect.[18],[19] If $C_{p_i} = (p_i - p_0)/q_0$ is the pressure coefficient due to the Newtonian impact pressure p_i, and p_c is the pressure relief due to centrifugal forces, then the net pressure coefficient C_p is simply

$$C_p = C_{p_i} - \frac{p_c}{q_0} = \frac{(p_i - p_c) - p_0}{q_0}, \tag{41}$$

where the net pressure p is specified by $p = p_i - p_c$. Also, when centrifugal forces are present the limit angle θ_u denotes the point of zero net pressure coefficient, and not the point of zero impact pressure coefficient as in the earlier discussion.

The Newtonian impact pressures are evaluated according to the methods given in Part II. The pressure relief p_c resulting from centrifugal forces is evaluated from the formula

$$p_c = \frac{\rho V_{s_c}}{R} \frac{}{\Delta C}, \tag{42}$$

where $\dot{m}$ = rate of mass flow through a streamtube at any point on the surface

V_e = effective velocity in a streamtube at any point on the surface

R = radius of normal curvature of the streamtube at any point on the surface.

ΔC = width of the streamtube (the height of streamtube is the body layer thickness which is described below)

In order to evaluate $\dot{m}$ and R for a body of revolution at angle of attack, the particle paths, or streamtubes, on the body surface must be determined. In the hypersonic approximation the shock wave may be imagined to wrap itself around the portions of the body which are subject, or exposed, to compression flow. On these portions of the body the flow is confined to a thin, high density layer which lies on the surface of the body and which, therefore, may be referred to as "the body layer." Neglecting friction, the total reaction of the body layer fluid on the surface, and of the forces acting on the fluid, must be normal to the surface. Hence, the principal normal (normal radius of curvature) and therefore the osculating plane at every point on a streamline must be normal to the surface. Thus the streamtubes are similar to the geodesic paths obtained for the constrained motion of a particle on a curved surface.[14] At each point along a streamtube the radius of curvature is directed along the inward normal to the surface—that is, along the vector n. The rate of mass flow $\dot{m}$ at any point on a body layer streamtube is obtained by finding the sum of all the particles which have previously entered the body layer along the particular streamtube.

Let the curve C, Fig. 16, denote a streamtube lying on the surface of the body and let the radius of normal curvature of the streamtube at the point P on the surface be denoted by R. Let the lines of curvature at P have the directions

given by the unit vectors t (maximum radius of normal curvature) and b (minimum radius of normal curvature), and let the curve C (that is, the streamtube) at this point make the angle γ with t --Fig. 16. According to Euler's theorem[18] it follows that

$$\frac{1}{R} = \frac{\cos^2 \gamma}{R_1} + \frac{\sin^2 \gamma}{R_2} , \tag{43}$$

where R_1 is the radius of principal normal curvature in the t -direction, and R_2 that in the b -direction. For a body of revolution, which will be the case treated here, t is tangent to a meridian and b is tangent to a circular parallel; and the meridians and parallels are the lines of curvature on the surface.[16] R_1 is the radius of curvature of the normal (meridian) section obtained by passing a plane normal to the surface and containing the axis of symmetry. R_1 is known immediately when the profile shape of the body of revolution is specified. R_2 may be determined by means of Meusnier's theorem (see page 505, Reference 15) which shows that

$$R_2 = \frac{r}{\cos \theta} , \tag{44}$$

where r is the radius of curvature of a circular parallel and θ is the angle between n and r (that is, θ is the direction of the tangent along a meridian). From (43) and (44) it follows that

$$\frac{1}{R} = \frac{\cos^2 \gamma}{R_1} + \frac{\sin^2 \gamma \cos \theta}{r} \tag{45}$$

is the relation for the radius of curvature of the streamline at any point on the surface of a body of revolution.

Consideration must next be given to the velocity V_s of the flow over the surfaces of the body which are exposed to compression flow. When a free stream particle strikes the body layer at a local point P (see Fig. 16), it loses its component of velocity normal to the surface at this point, while the velocity components in the tangent plane remain unchanged. Letting γ_n denote the angle between V_0 and n

(η_n is identical with η in Eq. (3)), it follows from (3) that $\cos \eta_n = \cos \alpha \sin\theta - \sin \alpha \cos \theta \sin \beta$. The normal component of velocity $V_0 \cos \eta_n$ is lost upon impact, and the fluid particle after impact at the point P is left with the velocity components along t and b unchanged. If the angle between V_0 and t is denoted by η_t and the angle between V_0 and b by η_b , it follows from (3) that

$$\cos \eta_t = \cos \alpha \cos \theta + \sin \alpha \sin \theta \sin \beta, \tag{46}$$

and

$$\cos \eta_b = \sin \alpha \cos \beta. \tag{47}$$

After impact the particle is left with the instantaneous velocity components $V_0 \cos \eta_t$ along t and $V_0 \cos \eta_b$ along b . The resultant velocity vector is of magnitude

$$V_{s_t} = V_0(\cos^2\eta_t + \cos^2\eta_b)^{\frac{1}{2}}. \tag{48}$$

It lies in the tb-plane and makes the angle γ with the vector t , where

$$\cos \gamma = \frac{V_0 \cos \eta_t}{V_{s_t}} = \frac{1}{\left[1 + \left(\frac{\cos \eta_b}{\cos \eta_t}\right)^2\right]^{\frac{1}{2}}}. \tag{49}$$

From the relation $\tan \gamma = \cos \eta_b / \cos \eta_t$ it follows that

$$\tan \gamma = \frac{1}{\cot \alpha \cos \theta \sec \beta + \sin \theta \tan \beta}. \tag{50}$$

Although a single particle after striking the body would continue its motion in the tangential plane formed by t and b , the actual flow of a continuous medium constrains the particles to follow a streamtube on the surface. In order to evaluate the effective body layer streamtube velocity, V_{s_e} , a relationship must be found between V_{s_e} and V_{s_t} or V_∞ Five postulations have been scrutinized:

Case 1. $V_{s_e} = V_0$

This is the most simple assumption and would overestimate the centrifugal force effects.

Case 2. $V_{s_e} = V_{s_t}$

This yields the result that each particle does accelerate along the body layer but the postulation does not give a velocity gradient in the body layer at each point.

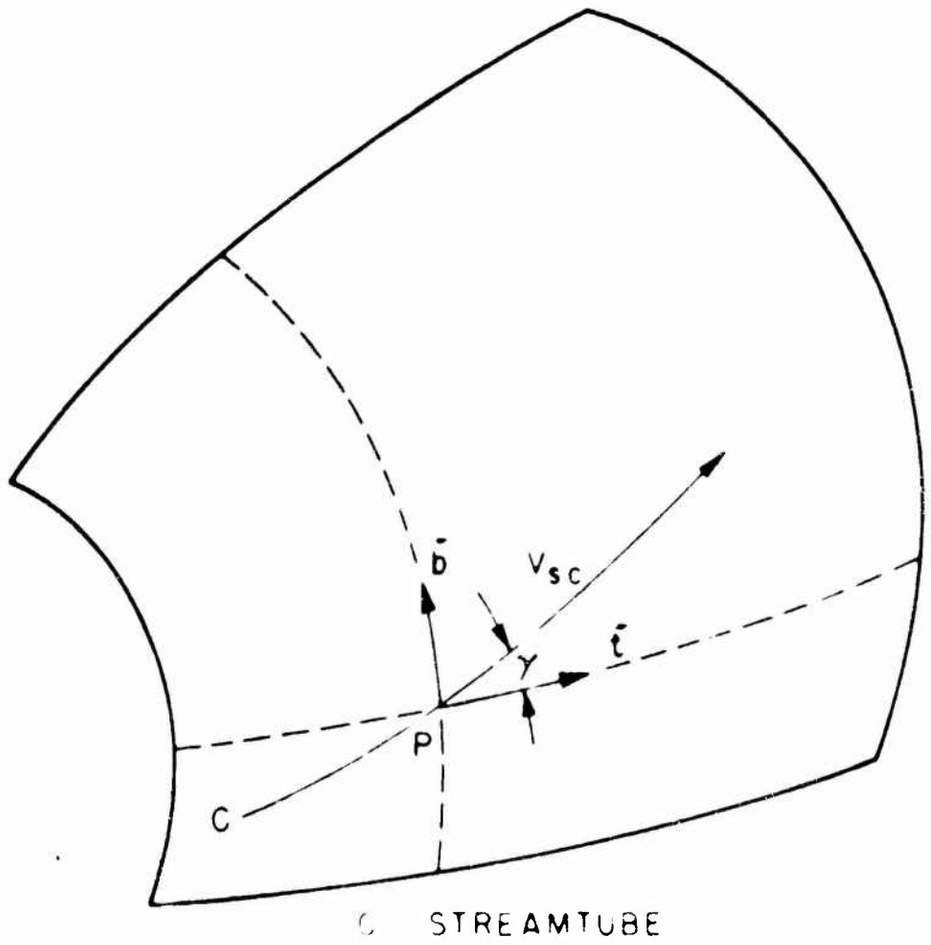

DIAGRAM OF STREAMTUBE ON SURFACE OF BODY

FIG. 16

P-87-8
P-87-8a

Case 3. $V_{s_2} = \int V_{s_1} dS / \int dS$

According to this method the velocity of a particle remains constant after impact, and results in the existence of a velocity gradient in the body layer (see Refs. 12, 13, 17, 18, and 19).

Case 4. $V_{s_2} = V_{s_1}/2$

This relation is the result of the assumption that the thickness of the body layer is of the order of magnitude of that of the boundary layer. The velocity distribution normal to the body surface is considered as a linear function of the distance from the surface throughout the body layer.

Case 5. $V_{s_2} = f(\theta, \beta, \alpha) V_{s_1}/2$

Upon examination of the pressure distribution as obtained by Sauer [20] using the method of characteristics for the A-4 nose at Mach numbers of 3.24 and 8.00 (see Fig. 17), it appears that the local pressure coefficient should decrease slower than any of the above four cases and that the location of zero pressure coefficient should occur at the position where the surface tangent is parallel to the free stream direction. Since Case 4 yields reasonable pressure variation at the start of the body layer it is used as a starting point for a fifth case. The present fifth case is then a modification of Case 4, where $f(\theta, \beta, \alpha)$ must be unity at the origin of the body layer, varies as a quadratic along the body layer, and approaches zero at the position where the surface tangent is parallel to the axis of the free stream. As an additional check on the validity of Case 5, all five cases are applied to flow over spheres (see Fig. 18). The aerodynamic drags are shown in Fig. 19 as the limiting values for the experimental data of

Charters.[81] Since the skin friction and base drags for spheres at high velocities are negligibly small, Case 5 appears best.

EXAMPLE OF APPLICATION--CYLINDER, CASE 5

The treatment of the hypersonic forces on a cylinder will be based on the assumption that the cylinder is infinite. In the case of an infinite cylinder the surface streamlines are all parallel. This condition makes unnecessary the determination of the individual streamlines in the calculation of the centrifugal pressure effects. The rate of mass flow in the body layer at any particular position on the surface of the cylinder, where the centrifugal pressure is desired, is

$$\dot{m} = \rho_0 V_0 A_{cap} = \rho_0 V_0 r \ell_s \sin\alpha \cos\beta = \rho_B \delta_B V_{e_c} \ell_s \sin\gamma, \tag{51}$$

where ℓ_s is a specified length of the infinite cylinder. From Eq. (45) the radius of curvature R of a streamline on a cylinder is (since $R_1 = \infty$ and $\theta = 0$ for a cylinder)

$$R = \frac{r}{\sin^2\gamma}. \tag{52}$$

The expression for the centrifugal pressure at a point on a cylinder is

$$p_c = \frac{\dot{m} V_{e_c}}{\ell_s R \sin\gamma}. \tag{53}$$

Combining (51), (52), and (53), the centrifugal pressure relation may be written

$$p_c = \frac{\rho_0 V_0 r \ell_s \sin\alpha \cos\beta \sin^2\gamma}{\ell_s \sin\gamma \quad r} V_{e_c} = \rho_0 V_0 V_{e_c} \sin\alpha \cos\beta \sin\gamma. \tag{54}$$

Employing Case 5, the effective surface velocity for a cylinder is

$$V_{e_c} = \tfrac{1}{2} \sin^2\beta + k_0 \frac{\cos\alpha}{\cos\gamma}, \tag{55}$$

since $V_{e_i} = V_0 \dfrac{\cos\alpha}{\cos\gamma}$ as given by Eq. 49

Now Eq. (54) may be written

$$p_c = \rho_0 V_0^2 \sin\alpha \cos\beta \sin\gamma \frac{1}{2} \sin^2\beta \frac{\cos\alpha}{\cos\gamma} = \frac{1}{2}\rho_0 V_0^2 \sin\alpha \cos\beta \sin^2\beta \tan\gamma \cos\alpha. \quad (56)$$

For a cylinder ($\theta = 0$) Eq. (50) yields

$$\tan\gamma = \tan\alpha \cos\beta, \quad (57)$$

and (56) becomes

$$p_c = \tfrac{1}{2}\rho_0 V_0^2 \sin^2\alpha \cos^2\beta \sin^2\beta = \tfrac{1}{2}q_0 \sin^2\alpha \cos^2\beta \sin^2\beta. \quad (58)$$

For a cylinder the impact pressure coefficient given by Eq. (5) is

$$C_{p_i} = 2 \sin^2\alpha \sin^2\beta, \quad (59)$$

and the net pressure coefficient is

$$C_p \equiv C_{p_i} - \frac{p_c}{q_0} = \sin^2\beta \sin^2\alpha (2 - \cos^2\beta). \quad (60)$$

The equation defining β_s is $C_p = 0$, or $\sin^2\beta_s = 0$. Thus, for a cylinder $\beta_s = 0°$ for all α.

From Eq. (6) the normal force coefficient corresponding to the surface of the cylinder exposed to compression flow is

$$C_N \equiv \frac{N}{q_0 \pi r_s^2} = -\frac{2}{\pi}\frac{l_s}{r_s}\int_{-\frac{\pi}{2}}^{0} C_p \sin\beta \, d\beta = \frac{72}{15\pi}\frac{l_s}{d_s}\sin^2\alpha \quad (61)$$

where r_s is the cylinder radius and $d_s = 2r_s$ is the cylinder diameter.

By comparing this result with formula (30) for the case in which the centrifugal forces are neglected it is found that

$$\frac{(C_N)_{\text{with centrifugal force}}}{(C_N)_{\text{Newtonian}}} = 0.900 \quad (62)$$

In Fig. 20 the effect of the various postulated V_{s_e} on the normal force for a cylinder is given.

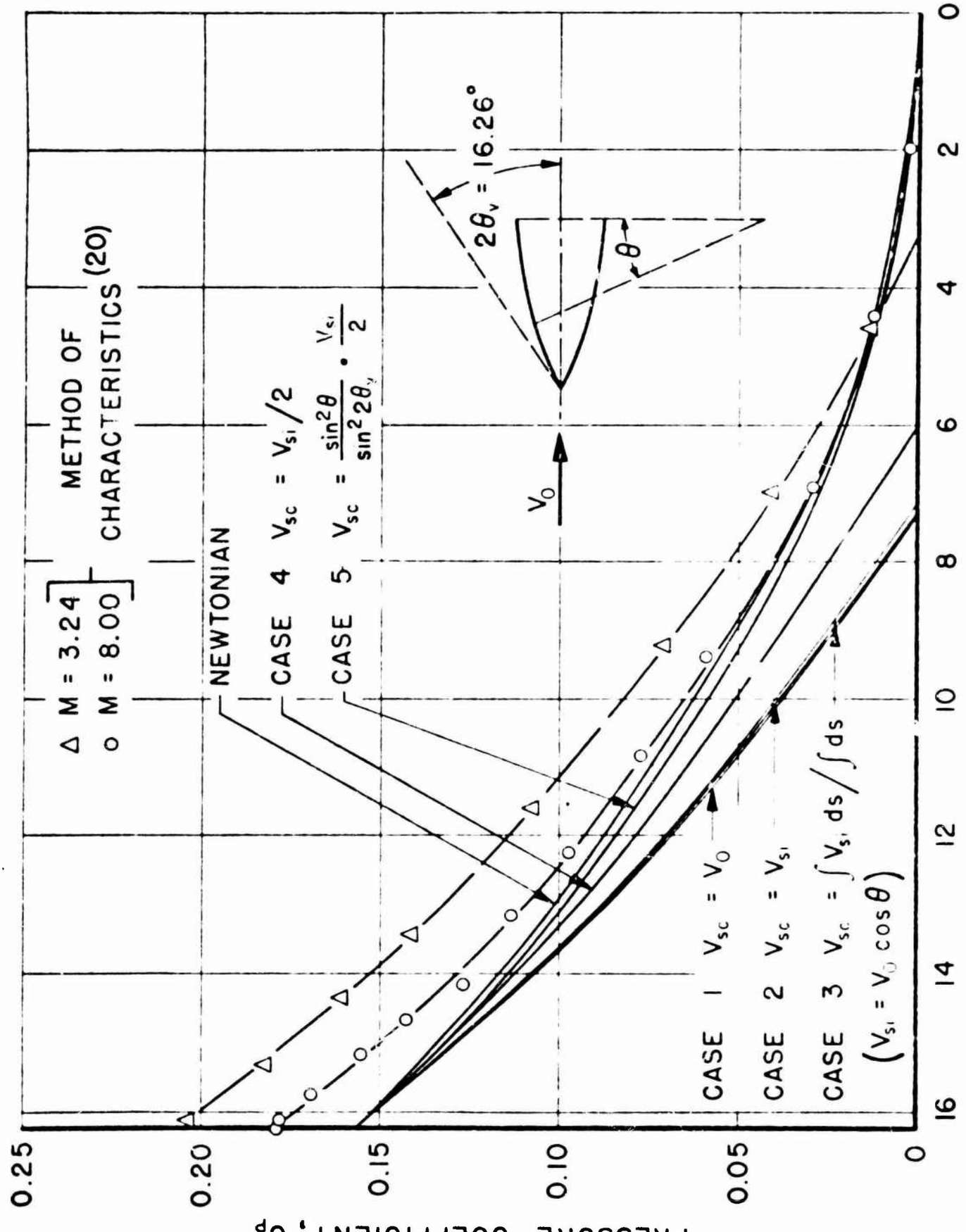

VARIATION OF PRESSURE COEFFICIENT ON NOSE OF A-4

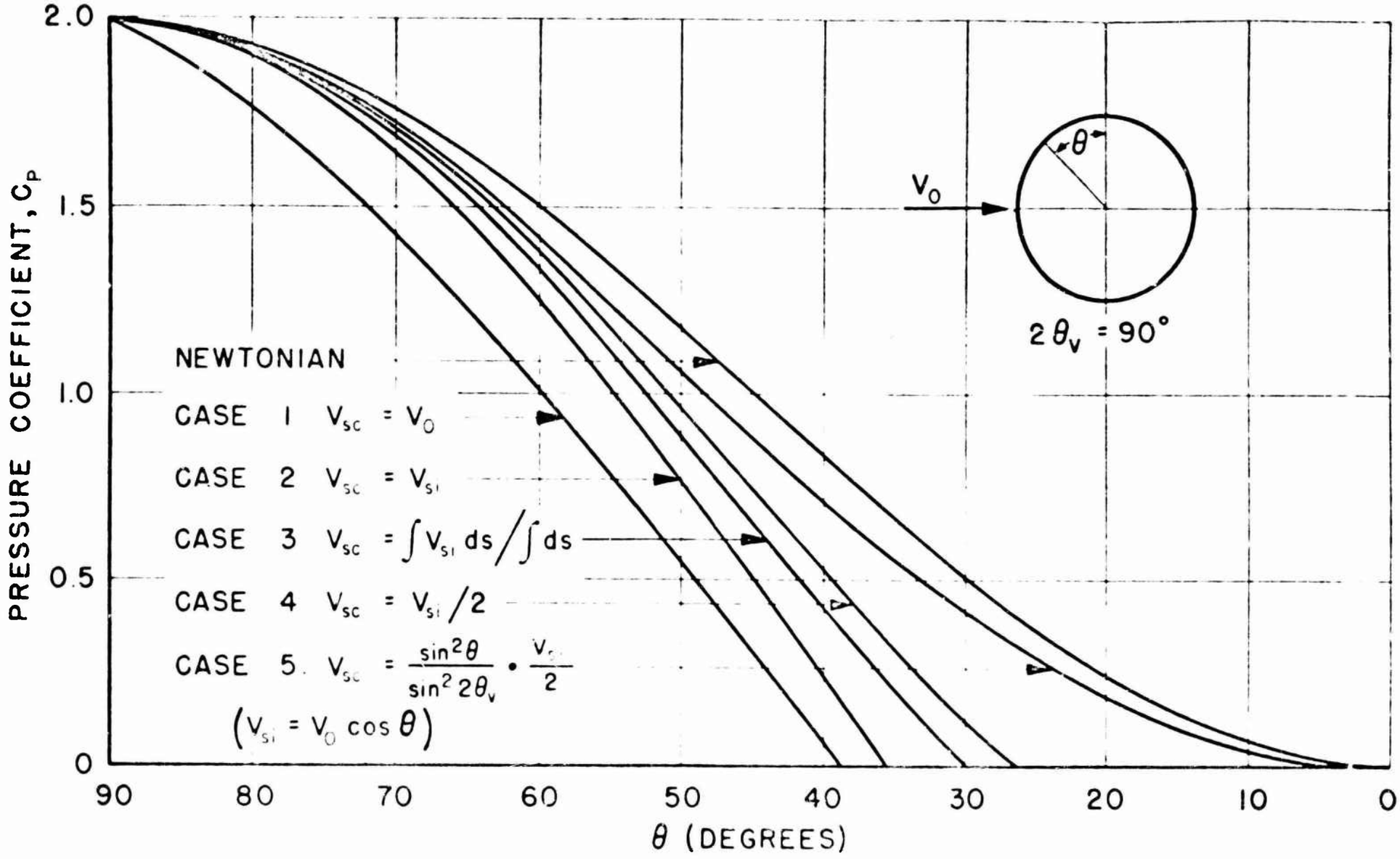

VARIATION OF PRESSURE COEFFICIENT ON A SPHERE

FIG. 18

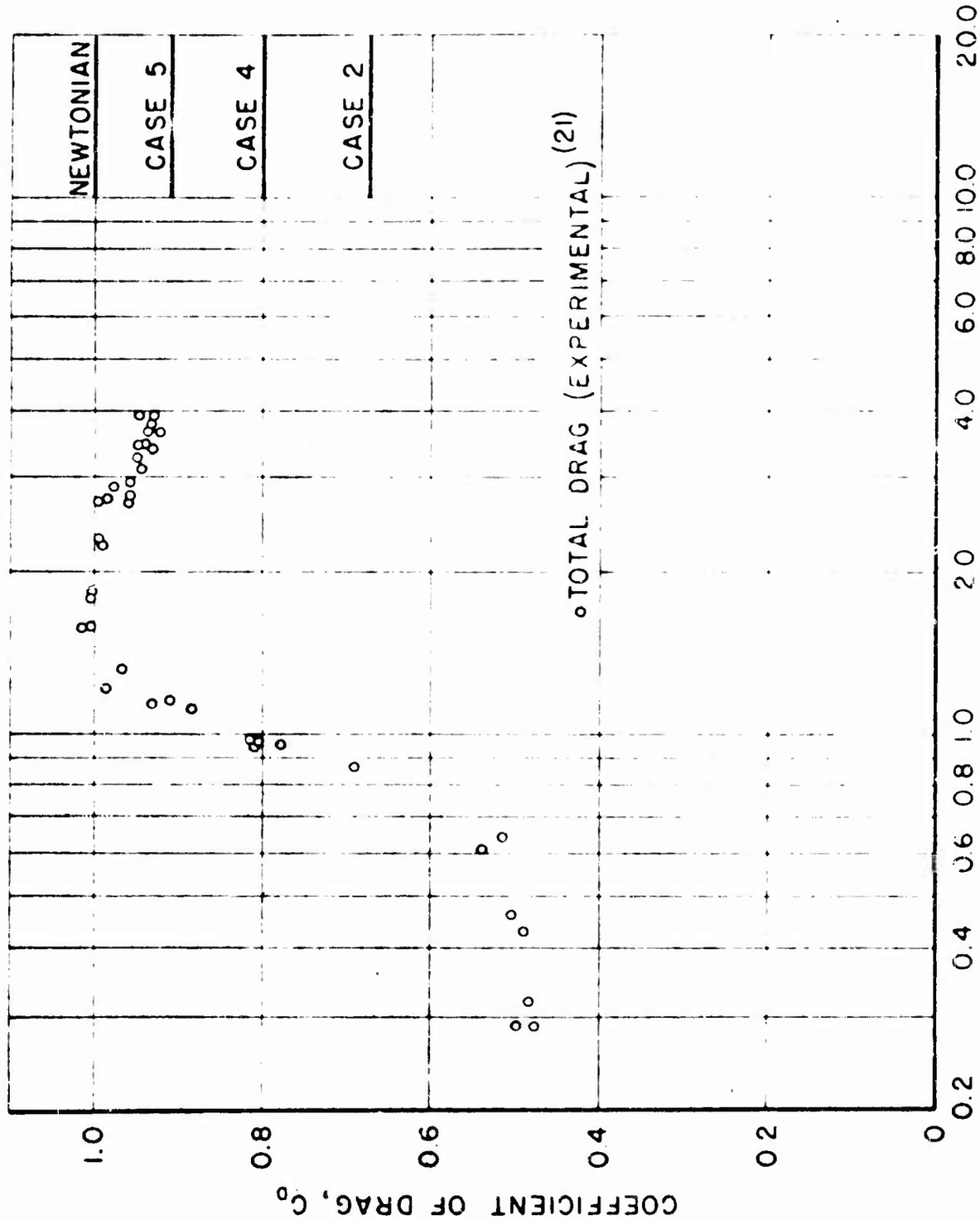

THE AERODYNAMIC DRAG ON SPHERES

FIG.19

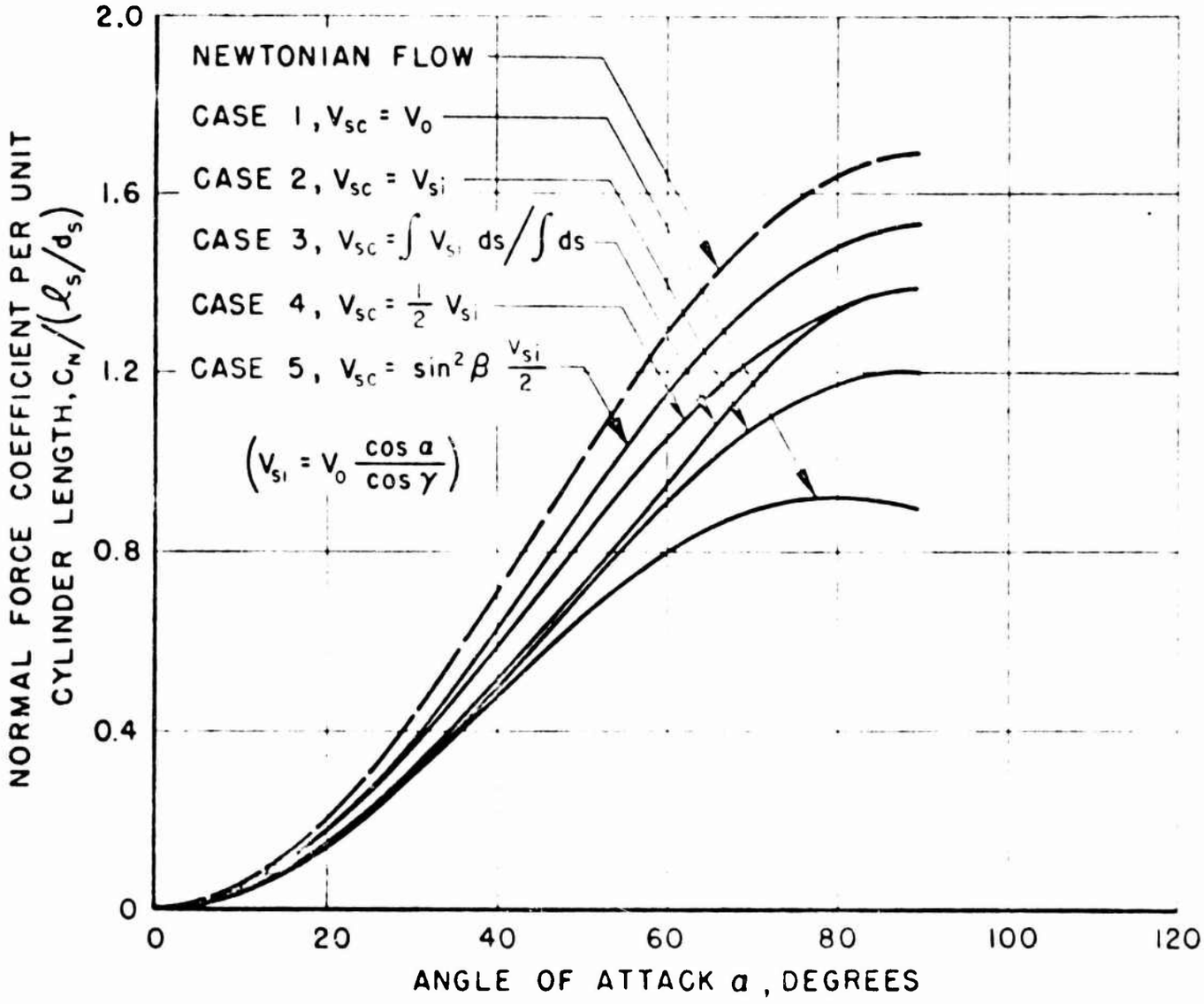

EFFECT OF V_{SC} ON THE NORMAL FORCE FOR A CYLINDER

FIG. 20

P-87-14a

REFERENCES

(1) A.H. Stone, "On Supersonic Flow Past a Slightly Yawing Cone," *M.I.T. Journal of Mathematics and Physics*, Vol.XXVII, No.1, April, 1948

(2) Z. Kopal, ed., *Supersonic Flow Around Yawing Cones*, M.I.T. Center of Analysis Technical Report No.3, 1947.

(3) A.F. Zahm, "Superaerodynamics," *J. Franklin Inst.*, Vol.217, No.2, February, 1934, p.153.

(4) P. Epstein, "On the Air Resistance of Projectiles," *Proc. Nat. Acad. Sci.*, Vol.17, No.9, September, 1931, pp.532-547.

(5) Th. von Kármán, "Isaac Newton and Aerodynamics," *J. Aero. Sci.*, Vol.9, No.14, December, 1942, p.521.

(6) E.V. Laitone, "Exact and Approximate Solutions of Two-Dimensional Shock Flow," *J. Aero. Sci.*, Vol.14, No.1, January, 1947, p.37.

(7) H. Erdmann, "Druckverteilungsmessungen am A4 VIP im Bereich der Unter- und Überschallgeschwindigkeiten," *Peenemünde Archiv* Nr.66/100.

(8) E. Herrman, "Druckverteilungsmessung am C2," *Peenemünde Archiv* Nr.66/136; "Vorläufiges Ergebnis der Druckverteilungsmessung am C2 des Projekts 'Wasserfall,'" *Peenemünde Archiv* Nr.66/146.

(9) Antonio Ferri, *Supersonic-Tunnel Measurements on Missiles*, NACA Wartime Report No.L-152, October, 1945.

(10) H. Walchner, *Systematic Wind-Tunnel Measurements on Missiles*, NACA TM No.1122, March, 1947.

(11) M.M. Munk, *The Aerodynamic Forces on Airship Hulls*, NACA TR No.184, 1923.

(12) A. Busemann, *Flüssigkeiten un Gasbewegung. Handwörterbuch der Naturwissenschaften*, Zweite Auflage, 1933, pp.275-277.

(13) H.R. Ivey, B.E. Klunker, and E.N. Bowen, "A Method for Determining the Aerodynamic Characteristics of Two- and Three-Dimensional Shapes at Hypersonic Speeds," NACA TN No.1613, July, 1948.

(14) W.D. MacMillan, *Theoretical Mechanics--Statics and Dynamics of a Particle*, New York: McGraw-Hill Book Company, Inc., 1927, pp.329-335.

(15) E. Goursat and E.R. Hedrick, *A Course in Mathematical Analysis*, Boston: Ginn and Company 1904, Vol.1, p.501.

(16) L.P. Eisenhardt, *A Treatise on the Differential Geometry of Curves and Surfaces*, Boston: Ginn and Company, 1909, p.126.

(17) H.R. Ivey and R.R. Morrissette, *An Approximate Determination of the Lift of Slender Cylindrical Bodies and Wing-Body Combinations at Very High Supersonic Speeds*, NACA TN No.1740, October, 1948.

(18) E. Sänger and J. Bredt, *Über einen Raketenantrieb für Fernbomber*, ZWB, UM Nr.3538, Berlin, 1944. Available as Navy Translation CGD-32, "A Rocket Drive for Long-Range Bombers."

(19) E. Sänger, "The Prospects of Jet Reaction Flight," *Interavia*, Vol.III, No.10, October, 1948.

(20) J.S. Iaenberg, *The Method of Characteristics in Compressible Flow, Part II*, Air Force AMC Technical Report TR 1173C, December, 1947.

(21) A.C. Charters, *Some Ballistic Contributions to Aerodynamics*, *J. Aero. Sci.*, Vol.14, March, 1947, p.155.